Quantitative Analysis of Aerosol Time-of-Flight Mass Spectrometry Data using YAADA

Contract Number 01-338

Final Report
May 14, 2004

Jonathan O. Allen

Department of Chemical & Materials Engineering
Department of Civil & Environmental Engineering
Arizona State University
Tempe, AZ 85287-6006

Prepared for the California Air Resources Board and the California Environmental Protection Agency

The statements and conclusions in this Report are those of the contractor and not necessarily those of the California Air Resources Board. The mention of commercial products, their source, or their use in connection with material reported herein is not to be construed as actual or implied endorsement of such products.

Acknowledgments

Prof. Kimberly Prather and her research group, then at the University of California, Riverside, participated in the Bakersfield Instrument Intercomparison Study (BIIS) in January 1999. David Suess and Jeff Whiteaker performed the field study and Jeff Whiteaker led the first analyses of these data. Prof. Prather and her research group have generously shared data from the BIIS experiment, as well as their expertise on operation of the ATOFMS instruments.

Reference sampler data from the BIIS were collected by Prof. Michael Kleeman at the University of California, Davis, and his group which includes Albert Chung and Jorn Herner. Prof. Kleeman has generously shared data from the BIIS experiment for the present project.

Dr. Prakash Bhave provided productive discussions and insightful suggestions regarding the development of YAADA, especially the YAADA Quantification Package. Dr. Bhave is a coauthor of the quant package for YAADA. He has already distributed two internal releases of this package to the coauthors and the Prather research group. He also provided extensive and very helpful comments on this report.

Dr. William Vance, Dr. Tony van Curen, and Dr. Nehzat Motallebi of the California Air Resources Board generously provided important comments on draft versions of this report. Dr. Motallebi offered essential aid and suggestions in her role as project manager.

This Report was submitted in fulfillment of Contract Number 01-338, *Quantitative Analysis of Aerosol Time-of-Flight Mass Spectrometry Data using YAADA*, by Arizona State University under the sponsorship of the California Air Resources Board. Work was completed as of 14 May 2004.

Contents

List of Figures

List of Tables

Abstract

Quantitative Analysis of Aerosol Time-of-Flight
Mass Spectrometry Data using YAADA

Aerosol Time-of-Flight Mass Spectrometry (ATOFMS) instruments have been used to measure the size and composition of single aerosol particles in California. ATOFMS data are not direct quantitative measurements of aerosol composition because the instruments exhibit non-linear response to aerosol concentration, particle size, and particle composition. The goal of this work is to quantitatively compare ATOFMS and reference sampler data in order to both understand ATOFMS instrument operation, and to develop procedures to transform ATOFMS data to semi-quantitative aerosol compositions. Ambient measurements from the Bakersfield Instrument Intercomparison Study were analyzed. ATOFMS instrument busy time (the time required to save acquired data) was found using a statistical comparison of the number of particles detected to that expected for a Poisson process modified to include busy time. The fraction of busy time was highly variable and in the range 0.05 to 0.95; thus busy time cannot be ignored for accurate quantitative comparison of ATOFMS data with reference sampler data. The sensitivities of the ATOFMS instrument to aerosol mass, organic carbon (OC), and elemental carbon (EC) were determined by a selecting single particle response function for each analyte. ATOFMS response to mass, OC and EC fit well to a power law in particle size; these responses are similar to those found previously for aerosol mass and inorganic ions. Using the recommended response functions, ATOFMS data were scaled for comparison with independent aerosol measurements. Comparison of scaled aerosol mass with that measured using Beta Attenuation Monitors (BAMs) showed semi-quantitative agreement, i.e., scaled ATOFMS data agreed within a factor of three with the BAMs data. ATOFMS data scaled for OC and EC concentrations were systematically lower than from collocated filter-based measurements because the scaled ATOFMS data propagated the systematic difference between short-term impactor measurements and the filter-based measurements. The novel data analysis methods developed here will be included in the next public release of YAADA, a software toolkit to analyze single particle mass spectral data.

Executive Summary

Background

Aerosol Time-of-Flight Mass Spectrometry (ATOFMS) instruments measure the size and composition of single aerosol particles. These instruments sample atmospheric aerosols and direct the flow through an expansion nozzle and skimmers [Noble and Prather, 1996, Gard et al., 1997]. During the expansion, particles are accelerated to a velocity characteristic of their aerodynamic size, with the smallest particles traveling at the highest speeds. After the last skimmer, velocities (hence aerodynamic size) of individual particles are measured by detecting scattered light from two timing lasers positioned a known distance apart. An ablation/ionization laser is then fired to intercept the moving particle. Ionized fragments from the particle are directed to positive and negative polarity time-of-flight mass spectrometers. Particles for which a mass spectrum is measured are referred to as *hit*, those particles for which size, but not a mass spectrum is measured are *missed*.

Numerous field study measurements with the ATOFMS instruments have provided continuous and detailed aerosol composition data for urban aerosols in California. For example, ATOFMS instruments have been used extensively to study the sources and transformations of urban atmospheric particles thought to affect human health [Gard et al., 1998, Hughes et al., 2000]. However, ATOFMS data do not directly provide quantitative information on aerosol composition because (1) the instruments require time to save particle data and this busy time increases with aerosol concentration, (2) particles are preferentially transmitted and detected based on their size [Allen et al., 2000a, Bhave et al., 2002], and (3) the laser ablation/ionization process used in ATOFMS instruments preferentially detects certain chemical species.

A number of investigators have studied the effect of particle composition on detection by laser ablation/ionization followed by mass spectrometry using laboratory-generated particles [Thomson et al., 1997, Neubauer et al., 1997, 1998, Ge et al., 1998, Kane and Johnston, 2000, Gross et al., 2000]. These investigators have shown that single-particle mass spectra are affected by the particle composition and size. In general alkali metal ions, ammonium nitrate, and aromatic organic compounds are efficiently ionized; aliphatic organic compounds are less efficiently ionized; ammonium sulfate is

poorly ionized [Kane and Johnston, 2000]. Ionization efficiency affects the minimum mass of a species that can be detected using ATOFMS; but, so long as some signal is detected, it is possible to determine the presence of the aerosol species using data analysis techniques that account for differences in ionization efficiencies. Gross et al. [2000], for example, demonstrated that the scaled response of alkali metals in mixed salt particles corresponds approximately to the relative composition in the particles.

Ammonium sulfate appears to be the main species that is not detected in ambient aerosols by ATOFMS as demonstrated by the results of the Atlanta Supersite Experiment in 1999 [Liu et al., 2003, Wenzel et al., 2003, Middlebrook et al., 2003]. Laboratory studies of ammonium sulfate particles have shown that these are less efficiently ionized in the presence of humidity sufficient to wet the particles [Neubauer et al., 1997, 1998]. The high humidity and high sulfate concentrations typical of Atlanta are not characteristic of conditions at Bakersfield, CA, in winter, so we have not attempted to account for missing aerosol ammonium sulfate in this work.

Much of the ionization efficiency literature is based on laboratory aerosols, which do not reproduce the composition and variety of ambient particles. We have made considerable progress towards characterizing the transmission efficiencies and chemical sensitivities of ATOFMS instruments for atmospheric particles by quantitatively comparing ATOFMS data with that from collocated reference samplers [Allen et al., 2000a, Bhave et al., 2002].

The goals of this work are first to develop an understanding of how ATOFMS instruments detect complex ambient particles, and second to use this knowledge to scale ATOFMS data back to ambient aerosol concentrations. As part of this first goal, we examined ATOFMS instrument busy time and its effect on particle detection. The ATOFMS instruments are busy and cannot detect new particles while particle size and composition data are saved by the data acquisition system. From laboratory measurements, the time to save missed and hit particle data were estimated to be ≈ 0.1 and 1.0 s, respectively. Characteristic rates of missed and hit particle detection for urban aerosols are 2 and 0.5 Hz, respectively; thus instrument busy time is expected to affect the ATOFMS detection rate, especially in times of high fine particle concentrations.

In the course of our earlier analysis of ATOFMS data, we developed YAADA, an object-oriented software toolkit to analyze single particle mass spectral data. YAADA is based on the insight that novel and efficient analysis of ATOFMS data sets is best done by programs written by researchers. In the programming model of data analysis, users develop and share code to document methods, share ideas, and collaborate. The novel data analysis methods developed here are implemented as functions in YAADA; the source code of these will be included in the next public release of YAADA.

Methods

As a result of earlier quantitative comparisons of ATOFMS and impactor data, the Prather group introduced a new data collection mode, *fast scatter*, in which the data acquisition system does not attempt to record mass spectra, minimizing instrument busy time. This mode was first used in the Bakersfield Instrument Intercomparison Study (BIIS) in January 1999. The ATOFMS instrument alternately acquired single particle composition and fast scatter data. These data were used to develop and test a new statistical method to determine ATOFMS instrument busy time directly. In this method, particle arrival rate is determined from the fast scatter data which have little or no busy time. Missed and hit particle data are then segregated and histogramed. These histograms are matched with Poisson with Busy Time distributions and the best-fit busy time parameters selected.

We have also generalized our method to compare ATOFMS and impactor data quantitatively using nonlinear regression. Critical to this method is the selection of single-particle response functions that relate ATOFMS measurements to aggregate aerosol composition. For comparisons of particle mass, the response function is simply the nominal particle mass. More difficult are response functions for aerosol components that are themselves operationally defined, including organic carbon (OC) and elemental carbon (EC). Response functions for OC and EC were based on classifications of particles detected by ATOFMS in studies of urban aerosol composition [Pastor et al., 2003]. The tested OC response functions used area of mass spectral peaks at $m/z = 27$ characteristic of $C_2H_3^+$ and/or $m/z = 43$ characteristic of CH_3O^+. Some response functions excluded mass spectra which resemble dust particles because of interference of Al^+ with $C_2H_3^+$. One group of EC response functions used the area of mass spectral peaks at $m/z = 36$ and 60 characteristic of C_3^+ and C_5^+. Another group of EC response functions used the ratio of peak areas characteristic of EC ($m/z = 36$ and 60) to the sum of peak areas characteristic of EC and OC ($m/z = 27$, 36, 43, and 60). Some response functions excluded mass spectra which resemble sea salt particles because of interference with large Cl^+ peaks which were detected at $m/z = 35$, 36, and 37.

Results

ATOFMS instrument busy time was found using a statistical comparison of the number of particles detected to that expected for a Poisson process modified to include busy time. This statistical approach was used to fit parameters in the equation

$$\text{BusyTime} = A\ \text{MissCount} + B\ \text{HitCount} + C\ \text{HitCount AvgFolderPos} \tag{1}$$

where BusyTime is instrument busy time in s; MissCount and HitCount are the number missed and hit particles in the period; AvgFolderPos is the average number of mass

spectra in the file folder when mass spectra were saved during the period. The last term in this equation accounts for the "folder-filling effect". The time to save a hit particle increases linearly with the number of spectra saved because each spectrum is saved as a separate file and the operating system requires time to verify the uniqueness of each file name. The best-fit busy time parameters indicate that the transportable ATOFMS used in the BIIS experiment took 0.17 s to save a missed particle, and between 0.32 and 1.21 s to save a hit particle. These parameters are significantly different from those determined by laboratory experiments in which particle events are simulated electronically.

Using busy time parameters from the field data, we calculated ATOFMS instrument busy times during BIIS. The fraction of busy time was highly variable and in the range 0.05 to 0.95. The resulting busy time scaling factors were also highly variable and in the range 1.0 to 20. Because of the large fraction of time the ATOFMS instrument spends processing data, busy time cannot be ignored for accurate quantitative comparison of ATOFMS data with reference sampler data. Busy time scaling is particularly important for urban aerosol data sets which can have large and rapid changes in concentration and composition.

We fitted the ATOFMS data for aerosol mass, OC, and EC to the matching reference sampler data using a power law dependence of ATOFMS response with aerodynamic particle size, D_a. ATOFMS data were transformed using a range of single-particle response functions. Response functions were selected based on goodness-of-fit to the power law dependence on D_a. The reference sampler data were size-segregated aerosol composition data collected for 7 intensive operating periods by Prof. Kleeman as part of the BIIS experiment. ATOFMS instrument responses for species i were compared with impactor data using the model $\alpha_i D_a^{\beta_i}$; the best-fit parameters and 95% confidence intervals for the analytes are

Analyte	α_i	β_i
Mass	1.9×10^3 [1.6–2.2 $\times 10^3$]	-5.7 [-6.0 – -5.4]
Organic Carbon	1.7×10^{-7} [1.4–2.1 $\times 10^{-7}$]	-3.0 [-3.4 – -2.7]
Elemental Carbon	2.4×10^{-5} [1.7–3.1 $\times 10^{-5}$]	-2.5 [-3.1 – -1.9]

The recommended OC response function was the area of mass spectral peaks at $m/z = 27$ excluding some mass spectra which resemble dust particles. The recommended EC response function used the ratio of peak areas characteristic of EC ($m/z = 36$ and 60) to the sum of peak areas characteristic of EC and OC ($m/z = 27$, 36, 43, and 60). The EC response function excluded mass spectra which resemble sea salt particles because of interference with large Cl^+ peaks. Using these response functions, the ATOFMS OC and EC data compared well with the impactor data. The comparisons are considered good because the scatter of the ATOFMS responses for OC and EC are similar to that for mass, suggesting that chemical sensitivity effects are less important for stable ATOFMS response than particle transmission effects.

Using the recommended response functions, ATOFMS data were scaled for comparison with independent aerosol measurements. Comparison of scaled aerosol mass with

that measured using a Beta Attenuation Monitors showed semi-quantitative agreement, i.e., scaled ATOFMS data agreed within a factor of three with the BAMs data. Scaled ATOFMS data for OC and EC were systematically lower than filter-based measurements; the scaled ATOFMS data propagated the systematic difference between short-term impactor measurements and the filter-based measurements.

Recommendations

Previous quantitative comparisons of ATOFMS and reference sampler data have either used busy times estimated from laboratory experiments or ignored busy time entirely. The present work demonstrates how representative fast scatter data can be used to determine ATOFMS instrument busy time directly from field study data. This procedure gives estimates of busy time that are both more accurate and significantly different from prior estimates.

The results of this work suggest several approaches to improve how busy time is accounted for in ATOFMS data. ATOFMS data can be scaled up to account for busy time, however, this method increases the sensitivity of the data to noise. Since the busy scaling factor is the inverse of the fraction of time that the instrument on-line, ATOFMS sampling of urban aerosols, for which the fraction of on-line time can be 5%, small perturbations in the calculated on-line time will lead to large changes in the busy scaling factor. We recommend the following methods to measure or calculate ATOFMS instrument busy time for future quantitative comparisons; in order of preference

1. Improve ATOFMS data acquisition hardware so that particle arrival rate is recorded continuously. This is equivalent to continuous acquisition of fast-scatter data.
2. Improve ATOFMS data acquisition hardware to record the amount of time that the ATOFMS is on-line, i.e. available to detect particle events.
3. Run ATOFMS instruments in fast scatter mode alternating with normal data acquisition mode.
4. Use busy time parameters developed from fast scatter data for a similar instrument during aerosol sampling.
5. Estimate busy time parameters from the maximum number of particle events of a given type detected in a period.

Since uncertainty regarding particle transmission and detection limits the precision of all quantitative comparisons of ATOFMS and reference sampler data, additional research in this area may improve quantitative analysis of ATOFMS data. Possible research projects in this area include laboratory studies of the transmission and detection of particles with known size and composition. Possible atmospheric sampling work includes

collection and analysis of collocated ATOFMS, scanning mobility particle sizer (SMPS), and aerosol particle sizer (APS) data.

Regarding single particle response functions, the mass spectral peaks that interfere with peaks characteristic of analytes will depend on the specific aerosol composition during a study. Subsequent studies should begin with the recommended single particle response functions developed here, and incorporate rules to exclude interfering ions specific to that study. These response functions can be evaluated qualitatively so that the chosen response functions have scatter approximately equal to that for the comparison of ATOFMS data with aerosol mass concentration. This is because the mass response function is based only on particle size, not mass spectral data, and so reflects uncertainty only in the transmission and detection of particles in the ATOFMS instruments. More quantitative measures of the goodness-of-fit for aerosol composition response functions are possible, but unjustified because uncertainties in transmission and detection will affect all response functions and response function performance with better precision than that for aerosol mass is likely coincidental.

In this study we observed that scaled ATOFMS data were systematically lower than independent filter-based measurements of fine aerosol OC and EC because OC and EC measured using an impactor were systematically lower than from filter-based measurements. The following recommendations are for subsequent collocated ATOFMS and reference sampler experiments:

- Samplers intended for use as reference samplers should have sampling protocols designed to detect aerosol analytes in quantities much greater than the limit of detection.
- Continuous samplers will be useful as reference samplers for quantitative comparison with ATOFMS data because 1-h measurements of aerosol composition provide a large number of data points for comparison.
- Elemental carbon is mainly emitted as particles which have $D_a \approx 100\ \mu$m. ATOFMS instruments should be improved to detect these small particles if semi-quantitative detection of EC is a goal. The ATOFMS instrument used in the BIIS experiment detected few particles smaller than $D_a = 0.32\ \mu$m.

ATOFMS instruments collect data in real time, but months or years have been required to develop conclusions from these studies. In order to study the sampled aerosol, the entire set of single particle mass spectra must be analyzed statistically; thus it is not surprising that ATOFMS data sets, which include 10^4–10^5 spectra per day of sampling, require considerable effort to analyze. We recommend streamlining ATOFMS data processing so that these data can be analyzed in real time.

A critical and time-consuming step in the analysis of ATOFMS data is the calibration of individual mass spectra. The mass spectra must be calibrated individually since the ablation position and space-charge effects of each particle result in non-uniform relation

between molecular TOF and mass-to-charge ratio. Currently, users generate calibrated peak lists using custom software for an entire study. These data are then saved to text files and imported batch-wise into YAADA. We propose to enhance YAADA so that ATOFMS data are transferred incrementally from the data acquisition computer to a data analysis computer over a network connection. The raw TOF data may then be calibrated automatically and incorporated into a data set for immediate analysis.

Chapter 1

Introduction

1.1 Single Particle Mass Spectrometry

An important new technology to measure atmospheric aerosols is single particle mass spectrometry (SPMS) which measures the composition of individual atmospheric aerosol particles [Noble and Prather, 2000, Johnston, 2000]. Since the macroscopic impacts of atmospheric aerosols on visibility and human health are strongly dependent on the composition of single particles, aerosol mass spectrometry has found wide application.

A commercially and scientifically successful SPMS design is Aerosol Time-of-Flight Mass Spectrometry (ATOFMS) developed by Prof. Kimberly Prather and her research group at the University of California, Riverside and later San Diego [Noble and Prather, 1996, Gard et al., 1997]. In California, ATOFMS instruments have been used extensively to study the sources and transformations of urban atmospheric particles thought to affect human health [Gard et al., 1998, Hughes et al., 2000].

ATOFMS instruments measure the size and composition of single particles in real time. These instruments sample atmospheric aerosols and direct the flow through an expansion nozzle and skimmers [Noble and Prather, 1996, Gard et al., 1997]. During the expansion, particles are accelerated to a velocity characteristic of their aerodynamic size, with the smallest particles traveling at the highest speeds. After the last skimmer, velocities (hence aerodynamic size) of individual particles are measured by detecting scattered light from two timing lasers positioned a known distance apart. An ablation/ionization laser is then fired to intercept the moving particle. Ionized fragments from the particle are directed to positive and negative polarity time-of-flight mass spectrometers. Particles for which a mass spectrum is measured are referred to as *hit*, those particles for which size, but not mass spectral data are captured, are *missed*.

ATOFMS instruments measure the size and composition of single aerosol particles, however, ATOFMS data do not provide direct quantitative information on aerosol composition. The analysis of ATOFMS data to quantitatively determine aerosol composition

presents these related challenges:

- ATOFMS instruments are unable to detect new particles while busy saving data; this busy time results in nonlinear response to ambient particle concentration.
- ATOFMS instruments preferentially transmit and detect particles based on their size [Allen et al., 2000a].
- The laser ablation/ionization process used in ATOFMS instruments preferentially detects certain chemical species [Gross et al., 2000].
- The data sets are large, approximately 200 megabytes/day, and heterogeneous.

In the present work we quantitatively compare ATOFMS data with aerosol mass and carbon concentrations from impactor samplers. The goal of this study is to understand the operation of ATOFMS instruments so that ATOFMS data can be scaled in order to provide continuous aerosol measurements. Such measurements are needed to better understand the sources, transformations, and fate of ambient particles in order to effectively regulate particulate matter and so mitigate effects on human health and regional visibility in California.

1.2 Field Studies in California

The first field study with the ATOFMS instruments was the 1996 Marine Particle Transport Study undertaken by the Prather group in collaboration with Prof. Glen Cass and his group at the California Institute of Technology. During this experiment, three ATOFMS instruments measured the size of approximately 3×10^6 particles and the composition of 3×10^5 particles. The total quantity of data collected during this and subsequent multi-day, multi-instrument studies has proven too large for *ad hoc* data analysis techniques. Since 1996, numerous design improvements to the ATOFMS have resulted in increased particle detection and hit rates so that the current data collection rate is 10^4 – 10^5 particle mass spectra per day; this is equivalent to $\approx 10^9$ bytes/day. Thus, the issues of ATOFMS data management and analysis require more attention as the number of ATOFMS instruments grows and their quality improves.

Since 1996, aerosol mass spectrometry has been used extensively in California to study the sources and transformations of urban atmospheric particles; Prof. Prather and her research group have participated in numerous field sampling studies including:

- Marine Particle Transport Study, Long Beach — Fullerton — Riverside, September — October 1996
- SCOS—NARSTO 1997 Radiation Study, Mount Wilson, June — July 1997

- SCOS-NARSTO 1997 Vehicle Study, Central LA — Azusa — Riverside, August 1997
- SCOS-NARSTO 1997 Nitrate Study, Diamond Bar — Mira Loma — Riverside, September — November 1997
- First Caldecott Tunnel Study, Orinda, November, 1997
- Vehicle Emission Study (Dynamometer), El Monte, July 1998
- Freeway Study, Riverside, July — August 1998:
- Bakersfield Instrument Intercomparison Study, Bakersfield, January 1999
- Ambient Monitoring, Riverside, October 1999 — April 2000
- Second Caldecott Tunnel Study, Orinda, July — August 2000
- EPA Supersite, Fresno, December 2000 — January 2001

The Prather group's extensive scientific publications arising from these field studies demonstrates the success of ATOFMS studies on the sources and fate of atmospheric aerosols in California [Noble and Prather, 1996, 1997, Liu et al., 1997, Gard et al., 1998, Gross et al., 2000, Silva and Prather, 2000, Guazzotti et al., 2001, Whiteaker et al., 2002, Whiteaker and Prather, 2003, Pastor et al., 2003]. More than 200 GB of ATOFMS data, much of it from urban sites in California, constitute an important resource for continuing study of particulate matter.

1.3 Prior Quantitative Comparisons of ATOFMS Data

ATOFMS instruments currently do not provide quantitative information on aerosol composition, but quantitative measurements are needed to better understand the sources, transformations, and fate of ambient particles, as well as the effects of particulate matter on global climate, human health, and regional visibility. Quantification of the chemical composition of individual laboratory-generated particles has been attempted [Mansoori et al., 1994, Ge et al., 1998, Gross et al., 2000], but the application of these techniques in field experiments is not yet possible because atmospheric aerosols are far more complex than laboratory-generated aerosols. Because we are interested in atmospheric aerosols, our efforts are directed toward quantitative analysis of field sampling data.

We have made considerable progress towards characterizing the transmission efficiencies and chemical sensitivities of ATOFMS instruments [Allen et al., 2000a, Bhave et al., 2002]. ATOFMS sampling alongside cascade impactors and laser optical particle counters during the 1996 field experiment [Hughes et al., 1999, 2000] provided data for

the calculation of ATOFMS particle detection efficiencies under ambient sampling conditions [Allen et al., 2000a]. Recently, chemical sensitivity calibrations were developed from collocated ATOFMS and impactor measurements taken during the 1996 and 1997 field experiments [Bhave et al., 2002]; this work used chemically-speciated size-resolved aerosol composition data from impactor measurements made in 1996 and 1997 [Hughes et al., 1999, 2000, Allen et al., 2000b, Hughes et al., 2002].

In the present work, we use different notation from that in Allen et al. [2000a] and Bhave et al. [2002]. These changes in notation are motivated by improvements in our methods as discussed at the end of this section. In the following discussion, notation from the original papers is used; thus notations are *not* consistent with each other or the present work. The notation from Allen et al. [2000a] is used in Equations 1.1–1.4; that from Bhave et al. [2002] is used in Equations 1.5–1.7.

In Allen et al. [2000a] and Bhave et al. [2002] we focused on the comparison of ATOFMS and collocated impactor measurements because aerosol concentrations measured using cascade impactor samples are the most direct method to determine the aerosol composition distribution as a function of particle size. Impactor data are particularly useful for the calibration of ATOFMS response because both the impactors and ATOFMS instruments segregate particles based on their aerodynamic diameters and operate over an overlapping aerodynamic size range, 0.32–1.8 μm. In Allen et al. [2000a], the aerosol mass concentration measured in sample i of a cascade impactor is designated m_i. The measured m_i is deemed to be the reference measurement of the aerosol mass during the impactor sampling period between the upper and lower cut-off diameters of the impactor stage.

In Allen et al. [2000a], we sum the responses of single particles detected in a sampling period and particle size range to determine the apparent aerosol concentration from ATOFMS data. The calculated mass of an ensemble of single particles detected by the ATOFMS was taken to be the apparent aerosol mass. Particles were assumed to be spherical and of uniform density, so that the apparent aerosol mass concentration in a narrow ATOFMS particle size bin j, m_j^*, was

$$m_j^* = n_j^* \frac{\pi}{6} \rho_p \overline{D_{p,j}}^3 \tag{1.1}$$

where ρ_p was the particle density and $\overline{D_{p,j}}$ was the logarithmic mean particle diameter in size bin j. The density of particles detected by the ATOFMS instruments was assumed to be 1.3 g cm^{-3}. The apparent aerosol number concentration in a particle size bin j, n_j^*, was calculated as the sum of particles hit by an ATOFMS in the size range $D_{a,j} < D_a < D_{a,j+1}$ divided by the volume of air sampled. This was corrected for ATOFMS instrument busy time using laboratory data to estimate busy time. For comparison with impactor data, the size range of particles included in each ATOFMS size bin j were conveniently chosen so that ten narrower ATOFMS bins fit within each impactor bin i. The ratio of the upper to lower particle size limit for each of these bins was approximately 1.06,

which was sufficiently small so that $\overline{D_{p,j}}$ was an accurate representation of particle size over the entire size bin.

The particle detection efficiency of an ATOFMS instrument in this paper was the ratio of aerosol mass as measured with a micro-orifice impactor (MOI) to that estimated from ATOFMS data, ϕ_{MOI}, calculated as

$$\phi_{\mathrm{MOI}} = \frac{m_i}{\sum_{j \subset i} m_j^*} \tag{1.2}$$

We then hypothesized that the ATOFMS particle counts can be reliably scaled by ϕ to yield atmospheric aerosol concentrations and that the scaling function is dependent only on D_a. This hypothesis was expressed as a testable model by rearrangement of Equation 1.2 to

$$m_i = \sum_{j \subset i} \phi(D_{a,j})\, m_j^* + \epsilon_i \tag{1.3}$$

where $\phi(D_{a,j})$ is the scaling function and ϵ_i is the residual aerosol mass concentration. Plots of ϕ versus D_a suggested that ϕ follows a power law relationship in D_a, i.e.

$$\phi = \alpha D_a^{\beta} \tag{1.4}$$

The observed power law dependence of particle detection efficiency on particle size was similar to that observed for particle transmission through supersonic expansion nozzles like those used in the ATOFMS instruments [Dahneke and Cheng, 1979]. Note that ϕ is the inverse of the particle mass detection efficiency.

Parameters α and β in Equation 1.4 were determined by nonlinear regression of impactor mass concentration data with apparent aerosol mass concentration determined from ATOFMS data. ATOFMS particle detection efficiencies did indeed display a power law dependence on particle aerodynamic diameter (D_a) over a calibration range of $0.32 < D_a < 1.8$ microns. Detection efficiencies were highest for the largest particles and decline by approximately two orders of magnitude for the smallest particles, depending on the ATOFMS design. Calibration constants developed in this paper are compared with those developed in the present work in Chapter 3.

Recently, ATOFMS chemical sensitivities were developed from collocated ATOFMS and impactor measurements taken during the 1996 and 1997 field experiments [Bhave et al., 2002]. In this work, intensities of selected peaks in individual particle spectra were related to the concentration of the corresponding aerosol species. These quantitative comparisons were then used to quantify NH_4^+ and NO_3^- concentrations in size-segregated ambient aerosols from ATOFMS data.

In Bhave et al. [2002], quantitative comparison of ATOFMS data with aerosol mass was first made to determine the transmission efficiency of the ATOFMS instrument for each intensive operating period. The modified regression model was

$$m_i = \sum_{j \subset i} \frac{\alpha D_{a,j}^{\beta}\, \frac{\pi}{6} \rho_p D_{p,j}^3}{V_i} + \epsilon_i \tag{1.5}$$

where the subscript j represents *individual particles* instead of an ensemble of particles with similar particle size (see Supplemental Material in Bhave et al. [2002]). The more direct regression on individual particles was enabled by improved computer hardware and software (YAADA). Equation 1.5 is comparable to Equation 1.3 after substitution for ϕ and m_j^*. As before, the volume of air sampled was corrected for ATOFMS instrument busy time using laboratory data to estimate busy time. The fitting parameters α and β were determined by nonlinear regression for each intensive operating period (IOP) of 2–4 d duration.

A regression model was then used to determine the sensitivity of the ATOFMS instrument for ammonium and nitrate as

$$m_{ik} = \sum_{j \subset i} \frac{\phi_j \, \mathrm{Resp}_{jk} \, \psi_{jk}}{V_i} + \epsilon_i \tag{1.6}$$

where the subscript k represents a chemical species, so m_{ik} is the concentration of species k in sample i. V_i is the volume of sampled air. The function $\phi_j = \alpha D_{a,j}^{\beta}$ accounts for the particle transmission efficiency; coefficients α and β fitted for each IOP were used here. The functions Resp_{jk} and ψ_{jk} account for the response and instrument sensitivity of particle j for species k, respectively. The response functions for ammonium and nitrate were the mass spectral response (sum of peak area) at $m/z = 18$ and $m/z = 30$, characteristic of NH_4^+ and NO^+, respectively. The instrument sensitivity was parameterized by a power law relationship in aerodynamic diameter

$$\psi_{jk} = \gamma_k D_{a,j}^{\delta_k} \tag{1.7}$$

Instrument sensitivities for both nitrate and ammonium showed a decrease with particle size, consistent with a decrease in the fraction of particle ablated and ionized for larger particles.

1.4 YAADA

ATOFMS Data sets from these multi-day studies have taken years to analyze. As part of our work to analyze ATOFMS data, we have developed YAADA, an object-oriented software toolkit that includes functions to import, query, and plot ATOFMS data. YAADA is based on the insight that novel and efficient analysis of ATOFMS data sets is best done by programs written by researchers. In the programming model of data analysis, users develop and share code to precisely document tasks, share ideas, and collaborate. This process is facilitated by specialized data analysis and plotting functions.

YAADA is implemented as a software toolkit written for Matlab (Mathworks, Natick MA), a programming environment widely used for scientific and engineering computation. The main components of YAADA import, query, and plot ATOFMS data. Some important features of YAADA are

- Data are stored in an extensible text file format that is suitable for archiving
- The import module rapidly performs quality assurance checks
- A custom query language is used to find particles which match some criteria
- A suite of plotting programs generate common plot formats

The original YAADA software was released to the Cass and Prather research groups in December 1999. Since then four stable versions of YAADA have been released which included additional functionality and better ease-of-use. YAADA has been used extensively to analyze ATOFMS data. Twelve graduate students in analytical chemistry and environmental engineering have produced numerous papers using YAADA since its initial development in the fall of 1999; a list of research papers developed using YAADA are listed on the website, http://www.yaada.org. Copyrights to YAADA are held by the California Institute of Technology and Arizona Board of Regents; both institutions have permitted free public use of the software including the source code. YAADA version 1.00a was released to the public as free software in December 2001.

1.5 Project Objectives

In the present work, we extend the quantitative comparison of ATOFMS and reference sampler data to determine ATOFMS transmission efficiencies and carbonaceous chemical sensitivities. The results obtained earlier [Allen et al., 2000a, Bhave et al., 2002] are based on few sampling days from IOPs in the 1996 field study at Long Beach and Riverside and the SCOS97 study at Riverside. Since 1996 substantial improvements have been made to the ATOFMS transportable instrument; they now detect both positive and negative ions and they now transmit a greater fraction of particles over a wider particle size range.

The present work is based on the hypothesis that ATOFMS data can be scaled to account for nonlinear particle and ion detection efficiencies to yield quantitative aerosol composition. Our earlier work encourages, but does not validate this hypothesis. Further work is needed to show that the scaling functions to account for particle detection and chemical sensitivity are applicable for a wider range of instrument operating conditions and aerosol compositions. If a general technique or set of scaling functions can be developed to scale ATOFMS data to quantitative aerosol compositions, then a large and growing data resource will be available to aid our understanding of the sources, transformations, and fate of ambient particles.

The original objectives of this study were

1. Compare quantitatively ATOFMS data and collocated impactor measurements of aerosol mass to determine particle detection efficiencies for the modified ATOFMS

design used in the Bakersfield Instrument Intercomparison Study (BIIS) and other studies.

2. Compare quantitatively ATOFMS data and collocated impactor measurements of aerosol carbon to determine chemical sensitivity of ATOFMS instruments for organic and elemental carbon in BIIS and other studies.

3. Develop, test, and distribute the quantification package for YAADA so that other users can perform quantitative comparisons of ATOFMS and reference sampler data.

We have completed Objectives 1 and 2, quantitatively comparing ATOFMS and impactor data from the BIIS field experiments. The programs used in this work will be packaged and documented for release with the final report. This will satisfy Objective 3.

As originally envisioned, the main work of this study was to explore the stability of particle transmission and chemical sensitivity scaling functions, including the stability of these functions over multiple field experiments. Instead, a large part of this study has been to determine ATOFMS instrument busy time using data from a single field study, BIIS.

Prior work had demonstrated the importance of ATOFMS instrument busy time. We found that existing parameterizations of ATOFMS busy time were not consistent with field sampling data, i.e., the parameterizations predicted greater than 100% busy time. This is of concern because, as part of the quantitative comparison, ATOFMS data are scaled by the inverse of the fraction of time on-line. A small inaccuracy in busy time could lead to the rejection of valid data if the calculated busy time exceeded 100% of the elapsed time; or worse, an erroneously large scaling factor if the calculated busy time approached the elapsed time, so that the inverse fraction of on-line time approached infinity. Thus, an accurate calculation of ATOFMS busy time is a critical first step to compare quantitatively ATOFMS and reference sampler data.

We developed a number of statistical approaches to determine ATOFMS instrument busy time from field sampling data. The final successful approach is described in the next chapter. This approach uses the *fast scatter* mode data which were first collected in the BIIS experiment.

We then determined ATOFMS instrument transmission efficiencies by comparing ATOFMS data with impactor mass measurements for the BIIS experiments. Comparisons of organic carbon (OC) and elemental carbon (EC) were also made using measures of ATOFMS response to particles containing OC and EC. These measures of response were suggested by Prof. Prather based on her group's extensive research.

Chapter 2

Busy Time

2.1 Background

The ATOFMS instruments process and save data on the size and composition of detected particles. During this time, the ATOFMS instrument electronic system is busy and cannot detect new particles. Instrument busy time alters ATOFMS instrument response so that changes in ambient particle concentration are not linearly propagated to the ATOFMS data. Correction for this nonlinear response is critical to accurate comparisons of ATOFMS and reference sampler data.

Consider the simple case that an instrument is busy for a fixed time, b, for each particle detected. The rate of arrival of particles at the instrument inlet, r_a, is expected to be directly proportional to the ambient aerosol concentration. However, the rate of particles detected, r_d, averaged over a sampling period is

$$r_d = r_a(1 - br_d) \tag{2.1}$$

where rates are given in Hz and busy time in seconds. Here r_d asymptotically approaches the maximum detection rate of $1/b$ and does not linearly respond to changes in ambient concentration (see Figure 2.1). As discussed below, ATOFMS busy time is more complicated than this simple case.

In 1998 David Fergenson, then with Prof. Prather's research group, ran laboratory experiments to estimate the factors which affect ATOFMS busy time [Fergenson, 1998]. In these experiments, hit and missed particle events were simulated electronically and the maximum rate of simulated event acquisition was measured. ATOFMS instrument busy times for missed particles were found to be constant. Hit particle busy times were longer than missed particle busy times and these times increased with the number of mass spectra saved in a computer file directory. These results were used to develop an expression to calculate ATOFMS instrument busy time:

$$\text{BusyTime} = A\ \text{MissCount} + B\ \text{HitCount} + C\ \text{HitCount AvgFolderPos} \tag{2.2}$$

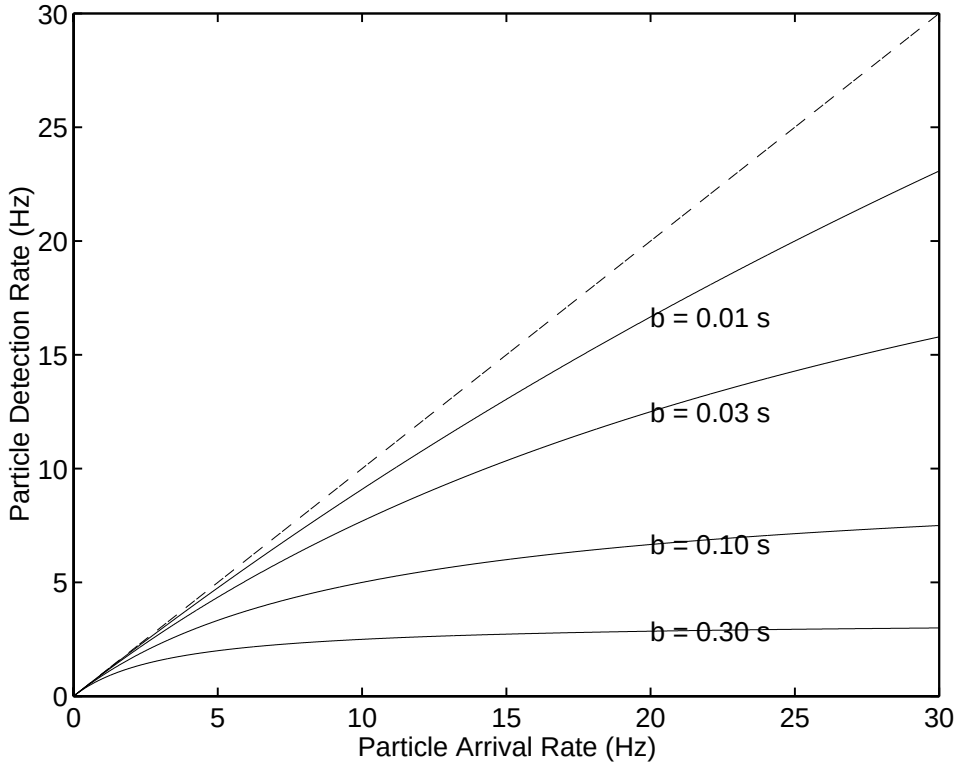

Figure 2.1: Response of particle detection rate in a hypothetical aerosol instrument to particle arrival rate for a range of instrument busy times. Instrument busy time per particle detected is b.

where BusyTime is instrument busy time in s; MissCount and HitCount are the number of missed and hit particles; AvgFolderPos is the average number of mass spectra in the file folder to which mass spectra were saved. The busy time parameters, A, B, and C, were determined from these experiments to be 0.255 s, 0.736 s, and 0.224 ms, respectively.

In our prior quantitative analysis of ATOFMS data [Allen et al., 2000a, Bhave et al., 2002], ATOFMS data were corrected for busy time. The time spent processing and saving data was calculated for each hour of the field experiment using Equation 2.2. ATOFMS particle counts for each hour were multiplied by a scaling factor to account for sampling time lost to instrument busy time and off-line time. The busy scaling factor, BusyScale, was calculated as

$$\text{BusyScale} = \frac{\text{SampTime}}{\text{SampTime} - \text{BusyTime} - \text{OffLineTime}} \tag{2.3}$$

where SampTime is the elapsed sampling time (1 h), and OffLineTime is off-line time.

Off-line time is calculated as the sum of periods 120 s or longer with no detected particles. Off-line time typically results from routine field maintenance of the ATOFMS,

for example cleaning the nozzles. The 120 s criteria was selected to capture these maintenance events, and not random periods of no particle events. The chance that a 120 s period has no particle events is very small ($\approx 5 \times 10^{-200}$) assuming a typical (low) arrival rate of 1 Hz (see Equation 2.4).

Note that as BusyTime + OffLineTime approaches SampTime, BusyScale increases without limit. The busy time parameters, A, B, and C, used in Allen et al. [2000a] and Bhave et al. [2002] were adjusted from the values determined in the laboratory experiment so that instrument busy time was less than $\approx$ 90% of on-line time for all sampling periods in the T96 and SCOS97 studies (see Table 2.1).

2.2 Methods

Fast Scatter Mode

Following analysis of ATOFMS data from the 1996 experiments and the simulated particle experiments described above, the Prather group implemented a new *fast scatter* data acquisition mode. In this mode, the data acquisition system did not attempt to acquire mass spectral data, thus minimizing instrument busy time. During the BIIS experiment, the Prather group operated the ATOFMS instruments in fast scatter mode for 5 min every 30 min. Below we demonstrate a technique to determine busy time parameters *directly* from field sampling data.

Regular cycling of the ATOFMS instrument between 5 min in fast scatter mode and 25 minutes in normal mode provides a continuous record of the arrival frequency of particles to the ATOFMS detection region throughout the BIIS experiment. A function, collect_fs, was written to collect fast scatter data and calculate the particle detection rate. This measure of particle detection rate varied over a hundred-fold range during the experiment with a maximum value greater than 50 Hz on 15 Jan 1999 and less than 0.5 Hz on 17-20 Jan 1999. Fast scatter particle detection rates show interesting short term features in the aerosol composition; for example, a rapid decrease in particle rate from $\approx$ 30 to $\approx$ 15 Hz in the early afternoon of 16 Jan 1999 (see Figure 2.2). This corresponds to a shift from stagnation to clear conditions identified using nephthelometer measurements [Whiteaker et al., 2002].

While the ATOFMS is operated, aerosol is continually drawn into the particle detection region. The arrival of these particles can be modeled as a Poisson process. Here the *arrival rate* is the frequency of particles which scatter light from both sizing lasers; in contrast, *detection rate* is the frequency of particles which scatter light from both sizing lasers *and are recorded*. A physical process can be described accurately as a Poisson process if (1) the number of events in each time period are independent, (2) the probability of an event is proportional to the length of the time interval, and (3) the probability of coincident events is small compared to the probability of single events

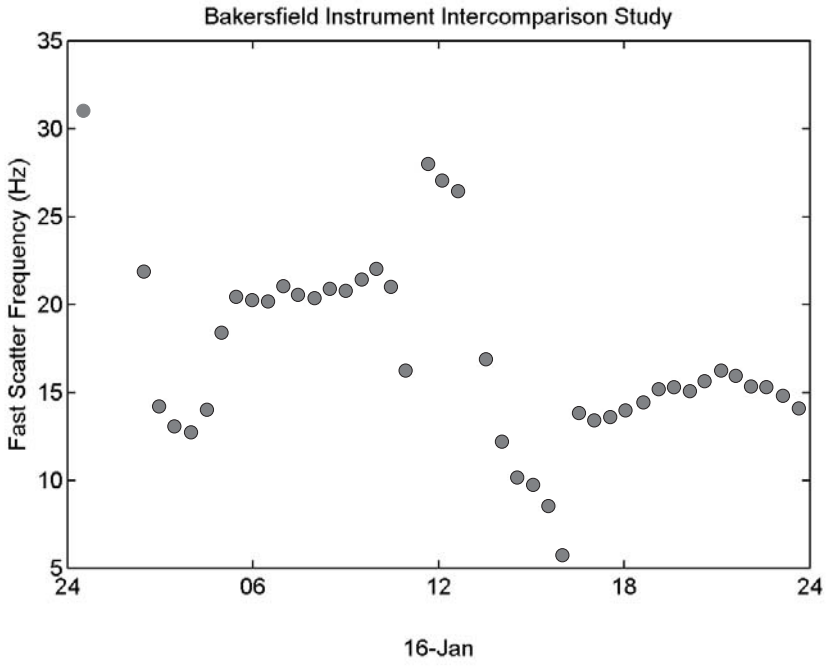

Figure 2.2: Fast scatter particle detection rate during 16 Jan 1999.

[DeGroot, 1986].

The first two conditions are met if the sampled aerosol is *uniform* over the sampling period. Since transmission of particles to the ATOFMS detection region has been shown to depend on particle size [Allen et al., 2000a] and may also depend on particle composition, the aerosol is uniform if the aerosol concentration, particle size distribution, and composition are approximately constant over the period of interest. For well-mixed ambient aerosol sampled for a sufficiently short time, the uniform aerosol assumption will be valid.

In order to use both fast scatter and composition data from the ATOFMS instruments, the minimum sampling period is the time for a complete cycle in the data acquisition modes, here 30 min. For analysis of these data as a Poisson process, the sampled aerosol must have approximately uniform composition over this period. As discussed below, data from periods which had substantially different fast scatter frequencies (see Figure 2.2) were not used in this analysis. Note that, the Poisson analysis is only needed to determine the busy time parameters, once these are determined, the full ATOFMS data set, including periods of rapidly changing aerosol concentration and composition, can be used to determine aerosol composition.

The third condition, that the probability of coincident events is small compared to the probability of single events, is equivalent to requiring that nearly all of the events are

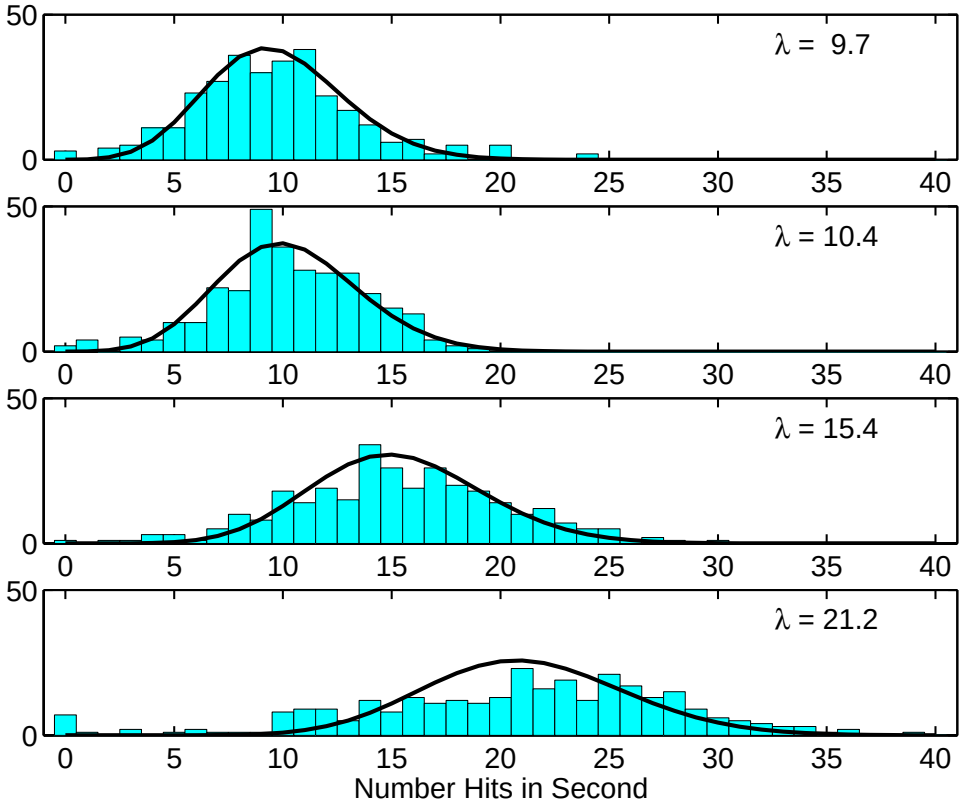

Figure 2.3: Histogram of number of particles detected in each second using fast scatter mode. Data collected in a sequence of four 5-min fast scatter operating periods starting at 0636, 0706, 0736, and 0806 hours PST on 14 Jan 1999. Fitted Poisson distributions are shown as lines. The fitted Poisson frequencies, λ, are also given for each period.

distinguished and recorded. This condition is not met in the case that the instrument is busy for a significant fraction of the sampling time.

In order to determine the arrival rate of particles to the ATOFMS detection region, we assume that the ATOFMS instrument busy time in fast scatter mode is negligible; this assumption is evaluated below. The measured mean from a Poisson distribution is an efficient estimator of, λ, the frequency of an event, here particle arrival [DeGroot, 1986]. The Poisson distribution probability function is

$$f(x) = \frac{e^{-\lambda}\lambda^{x}}{x!} \tag{2.4}$$

where $f(x)$ is the number of events in period x ($x = 1, 2, \ldots$). Particle events are recorded with a resolution of 1 s, so that it is convenient to let $f(x)$ and λ be the number of particle arrivals in a second.

The distribution of particles detected in each second using fast scatter mode can be compared with a Poisson distribution. Example distributions from the morning of

14 Jan 1999 are shown in Figure 2.3. These measurements include two 5-min periods, starting at 0636 and 0706, which have relatively low particle detection rates. The third and fourth periods, starting at 0736 and 0806, have higher particle detection rates; this is likely due to the accumulation of particles emitted during the morning rush hour. Histogramed data from the first three periods closely match the Poisson distribution (shown as a curve), including the asymmetric tailing behavior, i.e. a few seconds with large numbers of particles. The fourth period demonstrates a poor match between the fast scatter data and Poisson distribution. This poor match is likely because the ambient aerosol was not uniform during the 5-min sampling period; the histogramed data are consistent with superimposed Poisson distributions with different λ values.

The match between histogramed fast scatter particle data and Poisson distributions for the entire BIIS experiment is generally like that in the top three panels of Figure 2.3. The generally good match between these data and the Poisson distribution, is evidence that particle detection in fast scatter mode can be modeled as a Poisson process.

Busy time for an ATOFMS instrument in fast scatter mode can be estimated from the maximum number of particles detected in one second. For the fast scatter periods shown in Figure 2.3, the maximum number of particles detected in one second was 44; the maximum for the entire study was 58 particles in one second. One can estimate busy time per particle, b, as

$$b = \frac{1}{\text{MaxNumEvent} - 1} \tag{2.5}$$

where MaxNumEvent is the maximum number of events in a second; one is subtracted from MaxNumEvent to account for effects at the edge of a time period. The b value estimated from Equation 2.5 can be regarded as a maximum busy time for a particle. For fast scatter mode, instrument busy time is less than 0.0175 s per particle. For comparison, the maximum numbers of hit and missed particles recorded in one second during BIIS are 3 and 12, respectively. Thus, the busy time in fast scatter mode is significantly less than in normal mode, and this mode provides the best available approximation of the particle arrival rate.

Missed Particle Busy Time

We aim to use field sampling data in order to determine missed particle busy time. The use of field data rather than laboratory response to simulated particle events, is expected to provide more relevant busy time parameters. This approach is based on two assumptions; first the fast scatter particle detection rate is an accurate measure of particle arrival; and second, that instrument busy time follows the form of Equation 2.2. This second assumption is reexamined below.

As demonstrated in Fergenson's laboratory experiment, ATOFMS instruments require time, on the order of 0.1 s, to save missed particle data. Missed particle detection rate during BIIS was often in the range 1–3 Hz. Thus, busy time due to missed particle

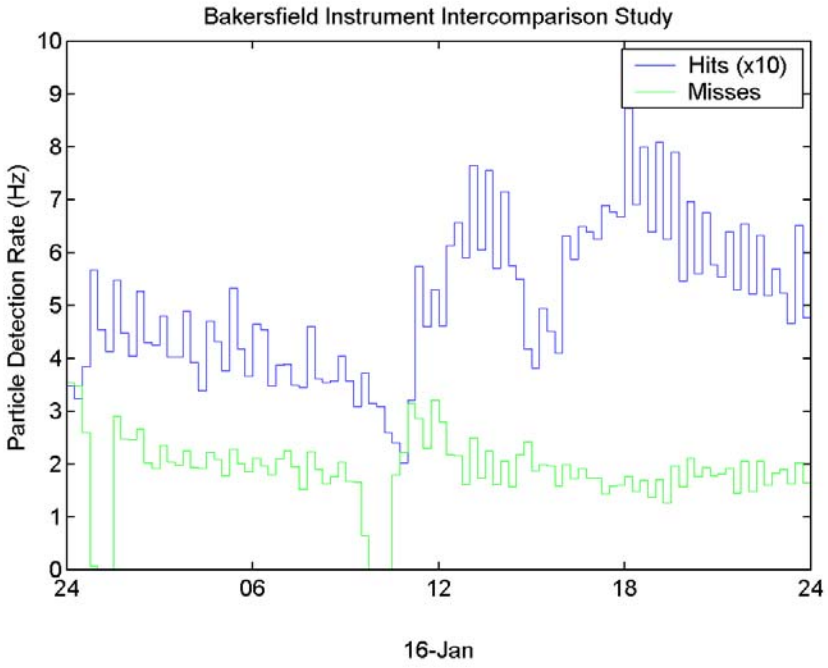

Figure 2.4: Hit and missed particle detection rate during normal ATOFMS data acquisition mode on 16 Jan 1999. The bar segments correspond to 15-min periods; the crenulation apparent in in these traces is the result of 5-min fast scatter periods which occur approximately once every 30 min.

acquisition is expected take ≈ 10–30% of available time and so have an important effect on instrument on-line time.

Comparison of particle detection rates is further evidence that instrument busy time significantly alters ATOFMS response to changes in ambient aerosols. Recall that on 16 Jan 1999, fast scatter particle detection rates are in the range 5–45 Hz and show interesting short term features (see Figure 2.2). In contrast, the rates of hit and missed particle detection are lower and have a lesser dynamic range than the fast scatter data (see Figure 2.4). On this day, the missed particle detection rate is in the range 1.3—3.3 Hz, and that for hit particle is 0.2–0.9 Hz. The missed particle detection rate is relatively featureless. The hit particle detection rate decreases in the late afternoon, at approximately 1600, at the same time that fewer fast scatter particles are detected. The maximum hit particle detection rate is in the early evening, at a time when fast scatter particle detection rate is approximately half of the maximum observed at noon. The early evening maximum in hit particle detection rate may be due to the presence of particles which were hit with greater probability than those sampled in the morning. Since the size of missed and hit particles are detected in the same way as fast scatter particles, if there were no instrument busy time, the sized particle detection rate (the

sum of missed and hit particle detection rates) would be equal to that for fast scatter particles. In fact, fast scatter detection rates are up to an order of magnitude greater than the sized particle detection rate.

In order to determine missed particle busy time, we segregated the ATOFMS data and considered only those missed particles expected to be unaffected by hit particle busy time. From prior laboratory experiments and analyses of field sampling data, the maximum hit particle busy time is approximately 1 s. This estimate is made using the busy time parameters measured in the laboratory (see Section 2.1) and the maximum number of mass spectra saved in a file folder (1000). The busy time of a hit particle sampled at the end of a second may therefore affect the fraction of on-line time in the next second. Therefore, in order to separate data not affected by hit particle busy time, only those seconds with no hit particles in *that or the prior second* are considered in the following analysis of missed particle busy time.

The number of missed, hit, and fast scatter particles detected in each second of a period were collected using the function collect_secbin. These data were then plotted as histograms which show the number of seconds which contain a specific number of missed particles. Comparative histograms of missed particles detected during a period of stable aerosol composition demonstrate the effect of hit particle busy time on the number of missed particles detected (see Figure 2.5). The number of seconds with zero or one missed particles is greatest for all seconds, lower for seconds with no hit particles, and a negligible fraction for seconds with no hit particles in that or the prior second. A histogram of missed particles with no hits in that or the *two* prior seconds (not shown) is similar to that in Figure 2.5c, but with significantly fewer seconds.

Missed particle data are segregated to remove the effect of hit particle busy time by considering only those missed particles detected in a second with no hit particles in that or the prior second. These data were then aggregated over a 25-min sampling period as a histogram of the number of seconds with a given number of missed particles (see Figure 2.5c). The observed missed particle histograms were then matched with synthetic particle histograms to determine the missed particle busy time, i.e. parameter A in Equation 2.2. The synthetic histograms were Poisson distributions modified to include busy time, called *Poisson with Busy Time* (PBT) distributions.

PBT distributions were generated by simulating particle events for 10^4 periods. Particles were randomly distributed with frequency λ, then particles which arrived during the busy time of a prior particle event were removed. PBT distributions were generated for values of particle arrival frequency, λ, in the range 0.1 to 1000, and per-particle busy time, A, in the range 0.001 to 1. Intermediate values of simulated A and λ were distributed logarithmically so that the relative difference between adjacent values was less than 5%. Units of A and λ depend on the length of the period; for the missed particle busy time, the period was 1 s, so the units of A and λ are s and Hz, respectively.

The best-fit busy time parameters were then found by matching observed missed particle histograms with the closest PBT distribution. Observed histograms were collected

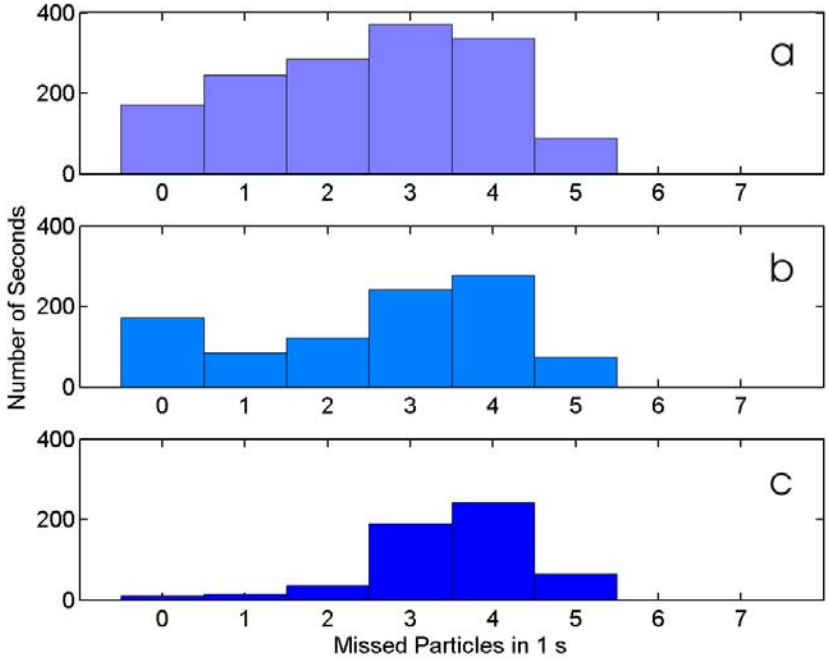

Figure 2.5: Histograms of missed particles detected in each second of the early morning (04:41-05:06) 12 Jan 1999; (a) all seconds, (b) seconds with no hits, and (c) seconds with no hits in that or the prior second.

from periods of normal ATOFMS operation which usually were 25 min. The particle arrival rates, λ, for the normal operating periods were taken to be the average particle detection rate measured in the fast scatter periods immediately before and after (see Figure 2.2). Data from normal sampling periods with a large difference (greater than 50%) in arrival rate between the preceding and following fast scatter periods were excluded because the aerosol composition was not stable and the assumptions underlying the analysis are not valid.

PBT distributions with λ closest to the fast scatter arrival frequency were compared with the observed histogram of particle events in order to determine per-particle busy time, A. The best-fit match was that with the minimum sum squared difference between the observed histogram and PBT distribution. The A for this PBT distribution is the best-fit parameter for this period. The matching procedure is shown graphically for two example periods in Figures 2.6 and 2.7. These periods were selected to include stable periods of high particle arrival rate, $\lambda \approx 27$ Hz at noon, and moderate particle arrival rate, $\lambda \approx 14$ Hz in early evening, on 16 Jan 1999. The best-fit A values for these two periods are representative of the range of values obtained for the study. Similar plots were generated and inspected for every 25-min sampling period over the study.

This matching procedure was repeated for the entire BIIS data set. The best fit

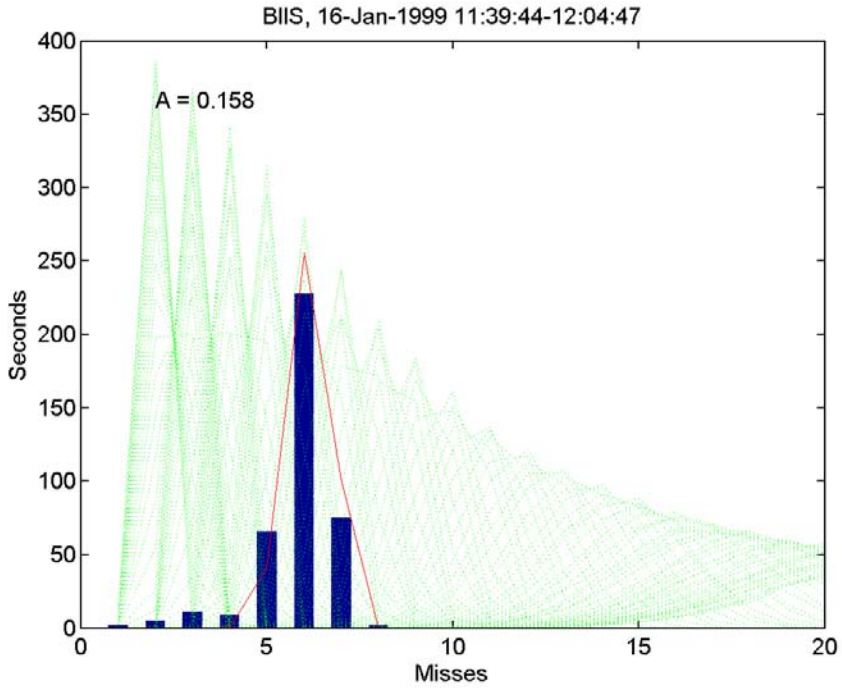

Figure 2.6: Match of observed missed particle histogram with Poisson with Busy Time distributions for midday (11:39-12:04) 16 Jan 1999. Observed particle histogram data are shown as bars. Poisson with Busy Time distributions have the frequency determined from fast scatter mode data, here ≈ 27 Hz. The solid line is the closest match among the PBT distributions; the corresponding busy time parameter, A, is given.

value of A for the entire study was found by summing the sum squared differences for each period over the entire study. The minimum value was 0.174 ± 0.008 s where the uncertainty is estimated from the precision of the PBT distribution parameters (≈ 5%). The best-fit value for the entire study was also the most common best-fit value for separate days of the study with sufficient particle arrival statistics (see Figure 2.8). This result supports the assumption that A is stable for the ATOFMS instrument over the entire BIIS experiment.

Hit Particle Busy Time

Our approach to determine hit particle busy times is similar to and builds upon the method used to determine missed particle busy times. Hit particle busy times are complicated by the folder filling effect. The time to save a hit particle increased linearly with the number of spectra saved in a file folder because each spectrum is saved as a separate file and the operating system requires time to verify the uniqueness of each file name. In the BIIS study, a maximum of 1000 spectra were saved in each folder. We

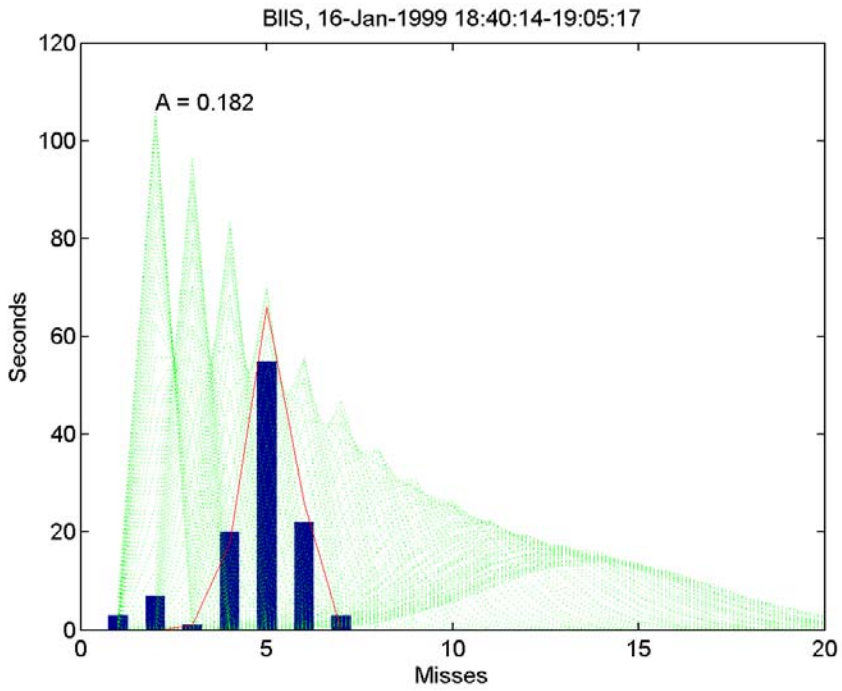

Figure 2.7: Match of observed missed particle histogram with Poisson with Busy Time distributions for evening (18:40-19:05) 16 Jan 1999. Observed particle histogram data are shown as bars. Poisson with Busy Time distributions have the frequency determined from fast scatter mode data, here $\approx$ 14 Hz. The solid line is the closest match among the PBT distributions; the corresponding busy time parameter, A, is given.

therefore segregate hit particles from missed particles, then further segregate hit particles by their position within the file folder ("folder position"). The collected hit particle data are then matched with the closest PBT distribution to find the best-fit busy time parameters.

During the BIIS experiment, the fraction of sized particles that were hit was in the range 10–35% with 15% a usual value. Because hit particles have a lower detection rate and longer busy times than missed particles, data periods longer than 1 s are needed to build hit particle distributions. Hit particle data were collected for 30 s periods; this time is exclusive of missed particle busy time. The 30 s period was selected as the shortest period for which the most likely number of hits was 3 for periods of relatively low hit particle detection, $\approx$ 0.1 Hz. A histogram with a maximum distribution at 3 was required for a distinct match with a PBT distribution; recall Figures 2.6 and 2.7.

As with the missed particle data, the hit particle data were aggregated over 25-min periods bounded by fast-scatter measurement periods. First, the number of missed, hit, and fast scatter particles were determined for each second. Then the fraction of each second spent as missed particle busy time was calculated using $A = 0.174$ s. Hit particle

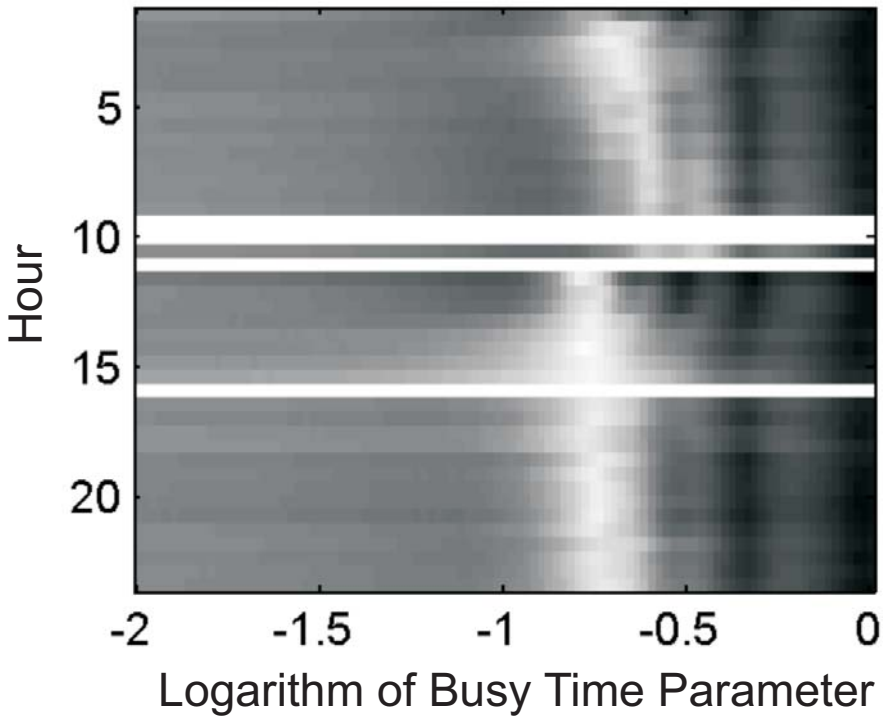

Figure 2.8: Sum of the squared difference for histogram matches for all periods during 16 Jan 1999. Periods within the day are shown as horizontal stripes marked by hour of day on the y-axis. The sum of squared residuals is shown as shades of gray; white corresponds to a good match.

data were then collected from sequential seconds so that the on-line time (exclusive of missed particle busy time) was between 30 and 31 s. The number of hit particles in these 30 s periods was then aggregated over a 25-min sampling period into a histogram of the number of 30-s periods with a given number of hit particles (analogous to Figure 2.5c).

Fast scatter detection rates were determined from data in the nearest fast scatter mode periods, exactly as was done for the missed particle busy time described above. The effective Poisson arrival rate, λ, was determined as the average fast scatter frequency (for 30 s) times the fraction of sized particles which were hit. Histograms of hit particle data were then compared with PBT distributions to find the best-fit hit particle busy time. The best-fit match was that with the minimum sum squared difference between the observed histogram and PBT distribution (analogous to Figures 2.6 and 2.7).

The best-fit hit particle busy times were expected to depend on folder position (see Equation 2.2). These fitted parameters for the entire BIIS experiment were collected based on their average folder position by binning average folder position into 10 folder position groups, i.e., 1–100, 101–200, ... 901–1000. The best-fit busy time parameters for the entire study tend to increase with folder position (see Figure 2.9). Note that the

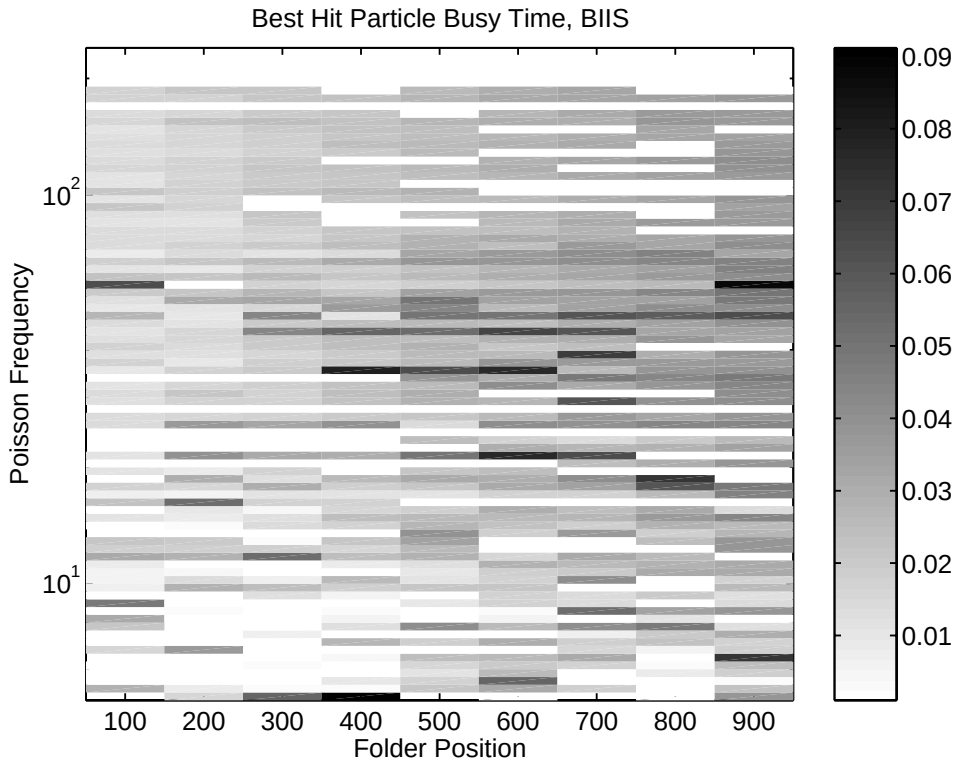

Figure 2.9: Best-fit hit particle busy time for combinations of λ and folder position for the entire BIIS experiment determined from matching hit particle histograms with Poisson with Busy Time distributions. The busy times, shown in the key on the right, are in fraction of the PBT distribution period, 30 s.

darker shades correspond to longer busy time and that the shading is darker for larger values of folder position. In this plot, best-fit busy time parameters are averages of all periods with the same frequency and folder position bins; scatter in this plot results because some of these bins include only a few 25-min sampling periods.

Best-fit hit particle busy times were aggregated by folder position. The median was used to aggregated these data since it minimized the effect of outliers. The aggregated hit particle busy times showed a linear dependence on folder position (see Figure 2.10). A linear fit of median busy time versus folder position yielded values for parameters B and C in Equation 2.2; these are 0.318 and 8.94×10^{-4} s. Busy times aggregated by averaging showed a similar linear dependence on folder position.

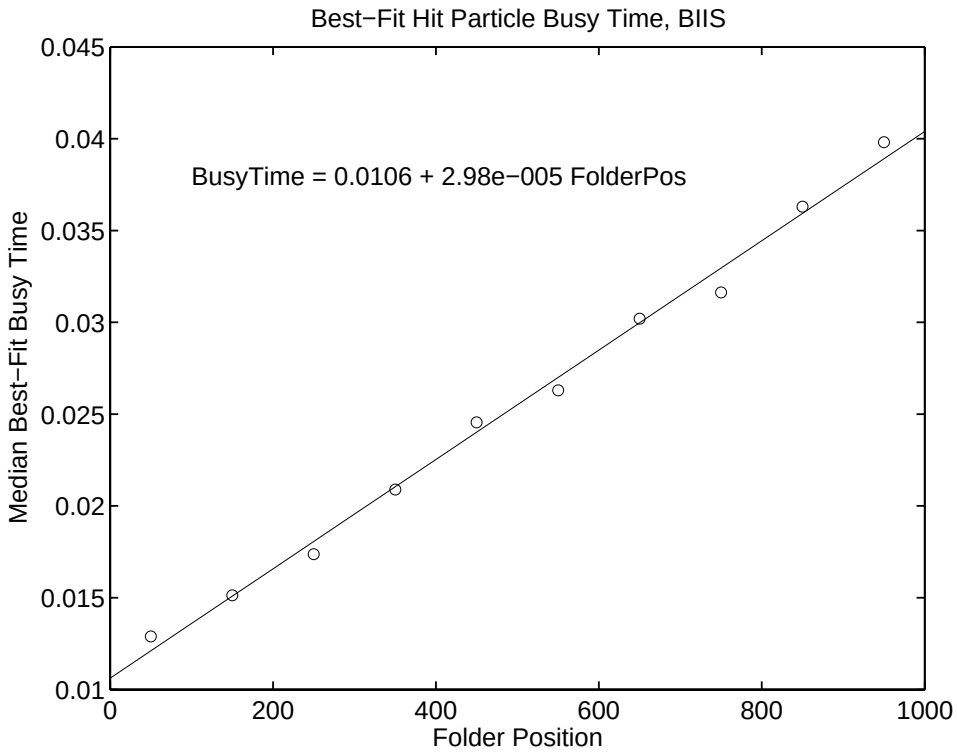

Figure 2.10: Median best-fit hit particle busy times for all λ values show a linear dependence on hit particle folder position. Fitted parameters of the busy time equation shown have units of the PBT distribution period, 30 s.

2.3 Results and Discussion

The motivation to develop busy time parameters from ATOFMS field sampling data was to scale ATOFMS data for busy time accurately. Using the parameters developed here, we can calculate BusyScale as

$$\text{BusyScale} = \frac{\text{SampTime}}{\text{SampTime} - \text{BusyTime} - \text{FastScatterTime} - \text{OffLineTime}} \tag{2.6}$$

This is analogous to Equation 2.3 with the addition of FastScatterTime. BusyTime is calculated from Equation 2.2, and OffLineTime is calculated as the sum of periods 120 s or longer with no detected particles. Fast scatter time is the sum of seconds in which fast scatter particles are recorded. On-line time is the remaining sampling time. The fraction of time that an ATOFMS instrument spent in these modes for 15-min periods is shown graphically in the lower panel of Figure 2.11. The inverse of the fraction on-line time is BusyScale (see top panel Figure 2.11. On this day the mass of fine particles was 51 μg m^{-3} [Chung et al., 2001]. BusyScale spans the range 1.5 to 12, and is a substantial correction to the apparent ATOFMS particle counts. These are typical values

Study	*A* (s)	*B* (s)	*C* (ms)
Lab Measurement Using Simulated Particles [Fergenson, 1998]	0.255	0.736	0.224
Estimated for 1996 Experiment Using Lab Measurements [Allen et al., 2000a]	0.130	0.634	0.167
Estimated for SCOS97 Experiment Using Lab Measurements [Bhave et al., 2002]	0.100	0.550	0.244
Statistical Analysis of BIIS Field Sampling Data (Present Study)	0.174	0.318	0.894

Table 2.1: ATOFMS Busy Time Parameters for BusyTime = *A* MissCount + *B* HitCount + *C* HitCount AvgFolderPos

for sampling during the BIIS experiment with moderate to high fine particulate matter concentrations.

The busy time parameters calculated here are significantly different from those developed in laboratory experiments and used in prior ATOFMS data analyses (see Table 2.1). In comparison with the laboratory measurements using electronically simulated particle events, the present parameters show a marked decrease in the time to save the first hit particle in a folder, but a more important effect of folder filling on busy time. These differences are likely due to a combination of 1) different data acquisition hardware and software between the laboratory and field experiments, and 2) the effect of actual particles on the entire ATOFMS instrument. In comparison with the values used by Allen et al. [2000a] and Bhave et al. [2002], the missed particle busy time calculated here is also much larger.

2.4 Conclusions and Recommendations

We have developed a new method to determine ATOFMS busy time from field sampling data which include fast scatter mode data. The results of this method yield consistent busy times which do not exceed the available time for any 15-min period in the BIIS experiment. The resulting busy time scaling factors are highly variable and in the range 1.0 to 20. Because of the large fraction of time the ATOFMS instrument spends processing data, busy time cannot be ignored for accurate quantitative comparison of ATOFMS data with reference sampler data. Busy time scaling is particularly important for ATOFMS data during sampling of moderate to high concentrations of fine particulate matter.

We recommend the following methods to measure or calculate ATOFMS instrument busy time, in order of preference,

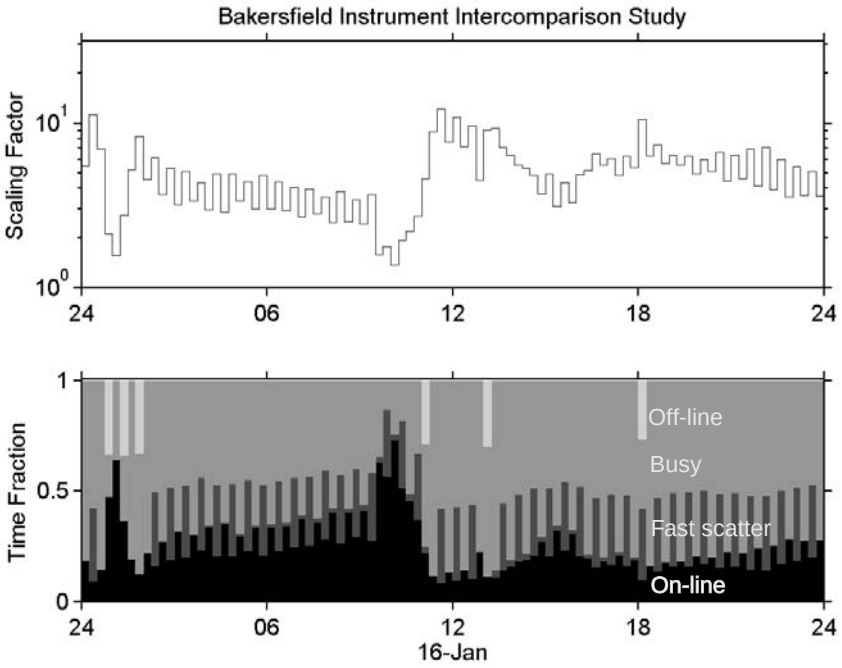

Figure 2.11: ATOFMS busy time and busy time scaling factors for 15-min periods during the BIIS experiment. Recall that fast scatter mode was run for 5 min every 30 min.

1. Improve ATOFMS data acquisition hardware so that particle arrival rate is recorded continuously. The particle sizing lasers are continuous lasers. The scattering signal from these lasers could be continuously recorded using a separate data acquisition stream. This is equivalent to simultaneous collection of fast scatter data that could be analyzed as discussed above. This recommendation was generated from discussions with Prof. Prather.

2. Record the amount of time that the ATOFMS waits between particle events using data acquisition hardware. These data would be a direct measure of on-line time.

3. Run ATOFMS instruments in fast scatter mode alternating with normal data acquisition mode. The procedure used for the BIIS experiment, with 5 min fast scatter data collection every 30 min, seems a good balance between these data modes.

4. Use busy time parameters developed from fast scatter data for a similar instrument during aerosol sampling.

5. Estimate busy time parameters from the maximum number of particle events of a given type detected in a period (see Equation 2.5).

While ATOFMS data can be scaled up to account for busy time, it should be noted that this method increases the sensitivity of the data to noise. For example, the effect

of an incorrectly sized particle collected during a period of high busy time would be magnified by the busy scaling factor.

Laboratory experiments using electronically simulated particle events have proven useful for establishing the functional form of ATOFMS busy time. Such experiments are also useful in the design and testing of data acquisition systems. However, the results of these experiments are inconsistent with field sampling data, i.e., these results predict more busy time than elapsed time, and therefore should not be used for scaling field sampling data.

Chapter 3

ATOFMS Response

3.1 Background

We calculated ATOFMS transmission efficiencies by quantitative comparison of ATOFMS and impactor data collected during the 1996 field experiment [Allen et al., 2000a]. In this work, transmission efficiencies were found to have a power law dependence on aerodynamic diameter (D_a), $\phi = \alpha D_a^{\beta}$, where α and β are coefficients determined from nonlinear regression. The observed power law dependence of particle detection efficiency on particle size is similar to that observed for particle transmission through supersonic expansion nozzles like those used in the ATOFMS instruments [Dahneke and Cheng, 1979].

We have also developed chemical sensitivity calibrations from collocated ATOFMS and impactor measurements taken during the 1996 and 1997 field experiments [Bhave et al., 2002]. In this work, intensities of selected peaks in individual particle spectra were related to the mass of corresponding chemical species in the bulk aerosol. These quantitative comparisons were then used to scale ATOFMS data to recover NH_4^+ and NO_3^- concentrations in size-segregated ambient aerosols. In this work, transmission efficiencies were first fitted to a power law using nonlinear regression similarly to the method used in Allen et al. [2000a]. ATOFMS instrument sensitivities for species k, ψ_k^{-1}, were then fitted to a power law dependence on aerodynamic diameter (D_a), $\psi_k = \gamma_k D_a^{\delta_k}$, where γ_k and δ_k are coefficients determined from nonlinear regression. Instrument sensitivities for both nitrate and ammonium showed a decrease with particle size, consistent with a decrease in the fraction of particle ablated and ionized for larger particles.

The objective of this work is to determine the particle detection efficiencies and chemical sensitivities of the ATOFMS instruments for carbonaceous aerosols by comparison with reference sampler data. In our prior work, particle detection efficiencies were determined by comparison of impactor mass and ATOFMS measurements while chemical sensitivities of NH_4^+ and NO_3^- were determined by comparison of impactor and

ATOFMS measurements of these species. Here we take a unified approach which can be applied to mass and chemical species measurements. We use the term *ATOFMS response* to include the combination of both particle transmission efficiency and chemical sensitivity.

3.2 Methods

Scaling functions for carbonaceous species detection efficiency are expected to be more complex than the prior work to quantify NH_4^+ and NO_3^- concentrations since elemental carbon (EC) and organic carbon (OC) are complex mixtures that are detected as a number of mass spectral peaks. EC and OC concentrations data for these comparisons are from thermal-optical analysis [Huntzicker et al., 1982, Birch and Cary, 1996] of samples collected on aluminum foil impaction substrates for the BIIS experiment [Chung et al., 2001].

During the BIIS experiment, impactors and ATOFMS instruments simultaneously measured the ambient aerosol composition during 7 intensive operating periods (IOPs) [Chung et al., 2001]. The IOPs were on 14 Jan 1999 (BAK01), 15 Jan 1999 (BAK02), 16 Jan 1999 (BAK03), 19 Jan 1999 (BAK04), 21 Jan 1999 (BAK05), 22 Jan 1999 (BAK06), 23 Jan 1999 (BAK07). The sampling period for IOPs BAK01-BAK06 was 1000–1800; for BAK07 it was 1000–1630. The overlapping ATOFMS and impactor data cover 3 size bins during seven IOPs, yielding a total of 21 reference measurements of up to 44 chemical species each. This is a relatively large available data set for developing ATOFMS chemical sensitivity calibrations.

Measurement of aerosol concentrations using cascade impactor samples is the most direct method to determine the aerosol mass distribution as a function of particle size. Impactor data are particularly useful for the calibration of ATOFMS response because both the impactors and ATOFMS instruments segregate particles based on their aerodynamic diameters and operate over an overlapping aerodynamic size range, 0.32–1.8 μm. The aerosol concentration of species i measured in sample j of a cascade impactor is designated m_{ij}. The measured m_{ij} is deemed to be the reference measurement of the aerosol mass during the impactor sampling period between the upper and lower cut-off diameters of the impactor stage.

The apparent aerosol concentration from ATOFMS data can be found by summing the responses of single particles detected in that time period and particle size bin. This apparent concentration of species i in sample j, m_{ij}^*, is corrected for busy time and calculated as

$$m_{ij}^* = \frac{\text{BusyScale}_j}{V_j} \sum_{k \subset j} R_{ik} \tag{3.1}$$

where V_j is the volume of sampled air, R_{ik} is the response of single particle k for aerosol component i. R_{ik} can be any function of the ATOFMS data which is expected to relate the

single particle data to the composition of the measured particle. Note that BusyScale_j is calculated from Equation 2.2 using the busy time parameters determined in the previous chapter. The BusyScale_j parameters and V_j are properties of the ATOFMS instrument in a sampling period; they are not affect by particle size.

A convenient measure of ATOFMS response is the ratio of aerosol component i as measured with an impactor to that estimated from ATOFMS data in sample j, ϕ_{ij}, calculated as

$$\phi_{ij} = \frac{m_{ij}}{m^*_{ij}} \tag{3.2}$$

Note that ϕ_{ij} is the inverse of the ATOFMS response to the sampled aerosol.

3.3 Results and Discussion

3.3.1 Aerosol Mass

The apparent mass of single particles detected by the ATOFMS is taken to be the single particle response for aerosol mass. If particles are assumed to be spherical and of uniform density, the single particle response is

$$R_{\text{mass},k} = \frac{\pi}{6}\rho_p D^3_{p,k} \tag{3.3}$$

where ρ_p is the particle density, $D_{p,k}$ is the physical particle diameter of particle k. The density of particles detected by the ATOFMS instruments is assumed to be 1.3 g cm^{-3}, a value between the densities of inorganic substances such as ammonium sulfate and the densities of organic liquids and water which have specific gravities close to unity. $D_{p,k}$ values were calculated from the measured aerodynamic diameters $D_{a,k}$ [Seinfeld and Pandis, 1998]. This R_{ik} is derived from ATOFMS measurements of single particle size (D_a) and is selected to be consistent with our earlier work [Allen et al., 2000a, Bhave et al., 2002].

Following our prior quantitative comparison work, we hypothesize that single particle ATOFMS data can be reliably scaled by a function ϕ_{ik} to yield atmospheric aerosol concentrations and that the scaling functions are dependent only on D_a. Note that ϕ_{ij} refers to an experimental measure of ATOFMS response efficiency, ϕ_{ik} refers to a single particle ATOFMS response efficiency, and ϕ without subscript refers to ATOFMS response efficiencies in general. These hypotheses can be expressed as a testable model by rearrangement of Equation 3.2 to

$$m_{ij} = \frac{\text{BusyScale}_j}{V_j} \sum_{k \subset j} \phi_{ik}(D_{a,k})\, R_{ik} + \epsilon_{ij} \tag{3.4}$$

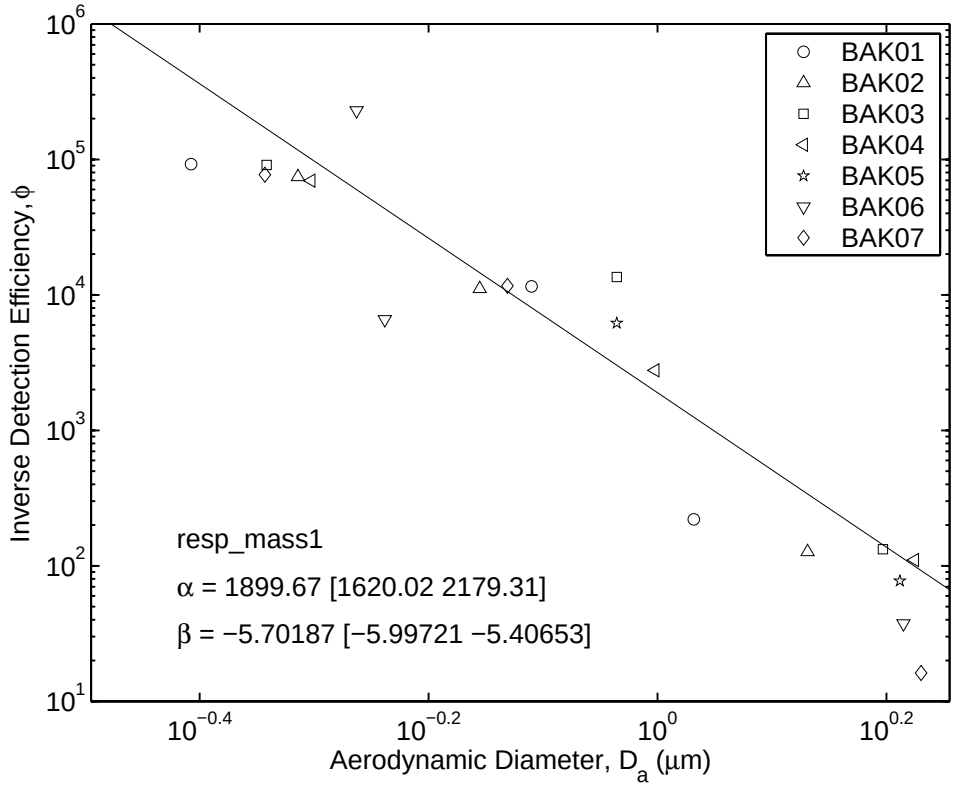

Figure 3.1: Inverse ATOFMS response efficiency, ϕ, versus aerodynamic diameter, D_a, for aerosol mass. Aerodynamic diameter is plotted at the average D_a weighted by the single particle response, R_{ik}. The line shows the best power law fit of the ATOFMS to impactor data. Text at lower left is single particle response function and fitted parameters; 95% confidence intervals are in brackets.

where ϵ_{ij} is the residual aerosol concentration. Plots of ϕ_{ij} versus D_a suggest that ϕ_{ik} follows a power law relationship in D_a (see Figure 3.1)

$$\phi_{ik} = \alpha_i D_{a,k}^{\beta_i} \tag{3.5}$$

The observed power law dependence of particle detection efficiency on particle size is similar to that observed for particle transmission through supersonic expansion nozzles like those used in the ATOFMS instruments [Dahneke and Cheng, 1979].

Parameters α_{mass} and β_{mass} in Equation 3.5 were determined by nonlinear regression of impactor mass concentration data on single particle ATOFMS data. Nonlinear regression analyses were conducted using the Levar-Marquardt algorithm [Press et al., 1992]. Fitted values of α_{mass} and β_{mass} are given in Table 3.1. Bracketed values show 95% confidence intervals for fitted parameters. The fitted scaling function is shown as a line on Figure 3.1. Recall that the values of ϕ_{ik} are single particle values, but are plotted in these figures as aggregated values located at the signal median diameter for each of the

impactor bins, but, in fact, values of m_{ik}^* are distributed over the entire width of their respective impactor bins. Since the single particle values were used in the regression analyses rather than the single average value represented by the symbols, the fitted curves do not necessarily pass through the symbols in these figures.

The fitted values of α_{mass} and β_{mass} compare well with these parameters fitted to 1996 data. In that study, quantitative comparisons were made to data from two transportable ATOFMS instruments; the α and β values from these two instruments are indistinguishable at the 95% confidence level from the present study. For the transportable ATOFMS instrument used in the BIIS experiment, analysis of data from the 1996 study yielded α_{mass} was 2133 ± 501 and β_{mass} was -5.527 ± 0.861.

As noted earlier [Allen et al., 2000a], the sampling biases shown in Figures 3.1 are advantageous for the accurate determination of aerosol concentration and chemical composition with the ATOFMS instruments. Because only a small fraction of the sampled aerosol particles can be sized and hit by the ATOFMS, sampling strongly biased against the more numerous smaller particles yields data on all particle size fractions. For a representative determination of aerosol mass concentration, it is convenient for the likelihood of sampling a particle to be proportional to the particle mass, i.e. approximately proportional to D_a^3, or $\phi \propto D_a^{-3}$. The effect of particle size on transmission observed in the BIIS data is more sensitive to particle size than this ideal sensitivity, so that particles in the lower range of particle size are detected with less than the ideal probability.

3.3.2 Organic Carbon

The single particle response for organic carbon (OC) is based on single particle mass spectral data. Bhave et al. [2002] used the mass spectral area of prominent ions characteristic of NH_4^+ and NO_3^- as the single particle response functions for these ions. For NH_4^+ we used $m/z = 18$ and for NO_3^-, $m/z = 30$ (NO^+). Unlike the inorganic ions, OC is composed of a heterogeneous mixture of chemical species from a number of sources, so that the single particle response for OC is not obvious.

Pastor et al. [2003] has reported on classes of particles observed using the ATOFMS instruments during SCOS97. We used the prominent ions from particle classes identified as "carbon" in whole or in part. Candidate ions (and their likely fragment ions) were $m/z = 27$ ($C_2H_3^+$, CHN^+) and $m/z = 43$ (CH_3O^+, $CHNO^+$). We examined various combinations of these candidate ions and attempted to exclude confounding mass spectral response in these definitions of single particle OC response, where response functions are designated **OC*x***,

OC1 Sum of peak areas with m/z in the range 26.5 to 27.5 (sum(Area{27})).

OC2 sum(Area{27}) excluding mass spectra which resemble dust particles. Mass spectra are excluded if sum(Area{1}), sum(Area{2}), sum(Area{39}), or sum(Area{40}) are

greater than sum(Area{27}). This condition is designed to exclude response due to Al^+ in dust particles (Classes 5, 6, 7, 10, 15, 18, 19, and 20 in Pastor et al. [2003]).

OC3 sum(Area{43})

OC4 sum(Area{43}) excluding mass spectra which resemble dust particles. Mass spectra are excluded if sum(Area{39}) is greater than sum(Area{43}). This condition is designed to exclude response due to dust particles (Class 7 in Pastor et al. [2003]).

OC5 sum(Area{27}) plus sum(Area{43})

OC6 sum(Area{27}) plus sum(Area{43}) excluding response due to dust particles as described for response functions OC2 and OC4.

OC7 sum(Area{27}) excluding mass spectra which resemble dust particles. Mass spectra are excluded if sum(Area{1}), or sum(Area{2}) are greater than sum(Area{27}). This condition is designed to exclude response due to Al^+ in dust particles (Classes 10, 18, 19, and 20 in Pastor et al. [2003]).

The response functions OC2, OC4, OC6 and OC7 are designed to exclude dust particles which have peaks at $m/z = 27$, likely due to Al^+, not OC components $C_2H_3^+$ and CHN^+. Particles are identified as "dust" particles using criteria based on soil dust clusters identified in Pastor et al. [2003]. Peaks at $m/z = 39$ and 40 are characteristic of K^+ and Ca^+; peaks at $m/z = 1$ and 2 are likely miscalibrated [Pastor et al., 2003], but are nevertheless characteristic of the response of ATOFMS instruments to soil dust particles. Note that sum(Area{x}) is the sum of peak areas with m/z between $x - 0.5$ and $x + 0.5$ mass units.

These single particle response functions were screened to eliminate those response functions with scatter greater than 2 orders of magnitude within an impactor particle size bin; OC5 and OC6 were removed from consideration for this reason. OC3 and OC4 were removed from consideration because fewer spectra contained a peak at $m/z = 43$ than $m/z = 27$. The fitted parameters using response functions OC1, OC2, and OC7 were similar. Among these OC7 was selected because some dust particles were excluded from consideration, but biomass burning particles were included. Particles from biomass burning are expected to contain both OC and K ($m/z = 39$). Particles of this type do not appear in the clusters developed by Pastor et al. [2003] because this source is insignificant when those data were collected (summer in Southern California).

Parameters α_{OC} and β_{OC} in Equation 3.5 were determined by nonlinear regression of impactor OC concentration data with single particle ATOFMS data. Nonlinear regression analyses were conducted using the Levar-Marquardt algorithm [Press et al., 1992]. Fitted values of α_{OC} and β_{OC} are given in Table 3.1. Bracketed values show 95% confidence intervals for fitted parameters. The selected scaling function is shown as a line in Figure 3.2.

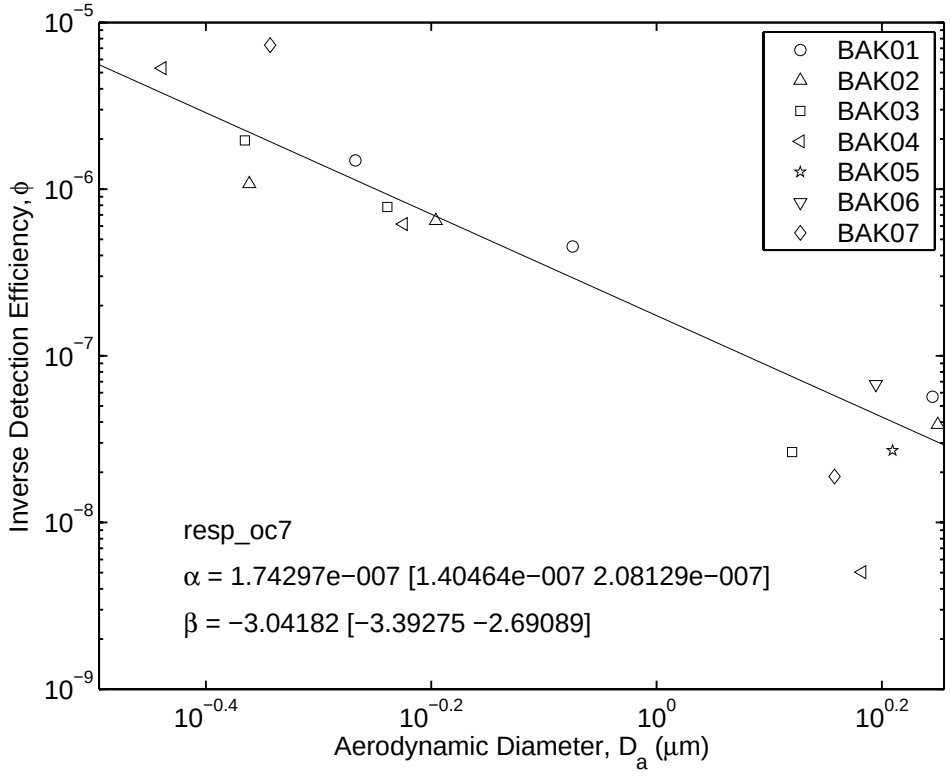

Figure 3.2: Inverse ATOFMS response efficiency, ϕ, versus aerodynamic diameter, D_a, for aerosol organic carbon using response function OC7. Aerodynamic diameter is plotted at the average D_a weighted by the single particle response, R_{ik}. The line shows the best power law fit of the ATOFMS to impactor data. Text at lower left is single particle response function and fitted parameters; 95% confidence intervals are in brackets.

The fitted value for β_{OC} is greater than that for β_{mass}. Thus, the ATOFMS instruments appear to be relatively more sensitive to OC in smaller particles than to OC in larger particles. This suggests that the laser ablation/ionization process does not sample the volume of the hit particles.

The fitted values of α_{OC} and β_{OC} can be compared with analogous parameters determined for inorganic ions by Bhave et al. [2002]. In that study single particle responses were scaled by $\phi\psi$ where ϕ was to account for transmission efficiency and ψ chemical sensitivity. Both ϕ and ψ were modeled as power law functions in D_a, as αD_a^{β} and γD_a^{δ}, respectively. The parameters from Bhave et al. [2002] can be combined so that $\alpha\gamma$ is compared with α_{OC} and $\beta+\delta$ is compared with β_{OC}. For NH_4^+ and NO_3^-, $\alpha\gamma \approx 10^{-6}$ and $\beta+\delta \approx -2$. The value for α_{OC} is an order of magnitude less than those determined for NH_4^+ and NO_3^-, indicative of greater ATOFMS response for OC as compared to these inorganic ions. Fitted β_{OC} is significantly lower than $\beta+\delta$ because the transportable ATOFMS used in the BIIS experiment has a sharper decrease in particle transmission

with particle size than the laboratory instrument whose data are the subject of Bhave et al. [2002]. The relative decrease in chemical sensitivity with size in these studies is similar with $\delta \approx 2.4$ in Bhave et al. [2002] and $\beta_{OC} - \beta_{mass} \approx 2.7$ in the present study.

3.3.3 Elemental Carbon

The single particle response for elemental carbon (EC) is also based on particle mass spectral data. As with OC, EC is not a single chemical species, but rather an operational definition of black carbon (soot). Using the classification of SCOS97 ATOFMS data [Pastor et al., 2003] we considered the prominent ions from particle classes identified as "elemental carbon" in whole or in part. Candidate ions (and their likely fragment ions) were $m/z = 36$ (C_3^+) and $m/z = 60$ (C_5^+).

We examined various combinations of these candidate ions and attempted to exclude confounding mass spectral response in these definitions of single particle EC response, where response functions are designated **EC*x***,

EC1 Sum of peak areas with m/z in the range 35.5 to 36.5, sum(Area{36}).

EC2 sum(Area{36}) excluding mass spectra which have relative area of peaks with m/z in the range 35.5 to 36.5, sum(RelArea{36}), less than 0.05. RelArea is the area of peaks divided by the total response (area) of all peaks in that spectrum. The relative area criterion is designed to include only particles with a strong elemental carbon signature.

EC3 sum(Area{36}) excluding mass spectra which have sum(RelArea{36}) < 0.10.

EC4 sum(Area{36}) excluding mass spectra which have sum(RelArea{36}) < 0.15.

EC5 sum(Area{36}) excluding mass spectra which have sum(RelArea{86}) > 0.02. This criterion is designed to exclude organic particles with amines which have characteristic peaks at $m/z = 86$ due to $[(C_2H_5)_2]^+$ (Classes 4 and 11 in Pastor et al. [2003]).

EC6 sum(Area{36}) excluding mass spectra which have sum(RelArea{86}) > 0.05.

EC7 sum(Area{36}) excluding mass spectra which have either sum(RelArea{36}) < 0.05 or sum(RelArea{86}) > 0.05.

EC8 sum(Area{36}) plus sum(Area{60}) excluding mass spectra which have sum(RelArea{36}) < 0.01 or sum(RelArea{60}) < 0.01 or sum(RelArea{23}) > 0.05. The sum(RelArea{36}) and sum(RelArea{60}) criteria are designed to include only those particles which have a significant EC signal. The sum(RelArea{23}) criterion is designed to exclude sea salt particles which have large peaks at $m/z = 35$ and 37 due to Cl^+; the chlorine peaks are often sufficiently large to carry over into $m/z = 36$.

EC9 Count of particles excluding those which have sum(RelArea{36}) < 0.01 or sum(RelArea{60}) < 0.01 or sum(RelArea{23}) > 0.05.

EC10 Ratio of peak areas characteristic of EC ($m/z = 36$ and 60) to the sum of peak areas characteristic of EC and OC ($m/z = 27$, 36, 43, and 60) excluding mass spectra which have sum(RelArea{36}) < 0.01 or sum(RelArea{60}) < 0.01 or sum(RelArea{23}) > 0.05.

EC11 Ratio of peak areas characteristic of EC ($m/z = 36$ and 60) to the sum of peak areas characteristic of EC and OC ($m/z = 27$, 36, 43, and 60).

Note that sum(Area{x}) is the sum of peak areas with m/z between $x-0.5$ and $x+0.5$ mass units. Note that sum(RelArea{x}) is the sum of peak areas with m/z between $x-0.5$ and $x+0.5$ mass units divided by the total area of all peaks in that mass spectrum.

Many of these single particle response functions resulted in scatter of approximately 2 orders of magnitude within an impactor particle size bin. The results from response function EC7 were typical of these EC response functions (see Figure 3.3). The relatively poor fit of elemental carbon detection efficiency using this and similar functions may be because elemental carbon in particles is coated by other material and the laser ablation/ionization process does not reliably sample the underlying EC core of these particles. This may be especially relevant for large particles in aged urban aerosols.

The response functions EC10 and EC11 take as the single particle response function, the ratio of peak areas characteristic of EC to those characteristic of total carbon. These response functions yield scatter in ϕ_{EC} comparable to that for aerosol mass and much less than the other EC response functions.

Parameters α_{EC} and β_{EC} in Equation 3.5 were determined by nonlinear regression of impactor mass concentration data on single particle ATOFMS data. Nonlinear regression analyses were conducted using the Levar-Marquardt algorithm [Press et al., 1992]. Fitted values of α_{EC} and β_{EC} using EC10 are given in Table 3.1. Bracketed values show 95% confidence interval of fitted parameters. The fitted scaling function is shown as a line in Figure 3.4.

The fitted values of α_{EC} and β_{EC} can be compared with analogous parameters determined for organic carbon discussed above and inorganic ions by Bhave et al. [2002]. In comparison with other values of α, α_{EC} is significantly larger since the response function is a relative peak area, not a peak area. The β_{EC} is comparable with values of β for other analytes.

3.4 Conclusions and Recommendations

We have developed a generalized method to compare ATOFMS and impactor data from ambient sampling experiments quantitatively. Critical to this method is the selection

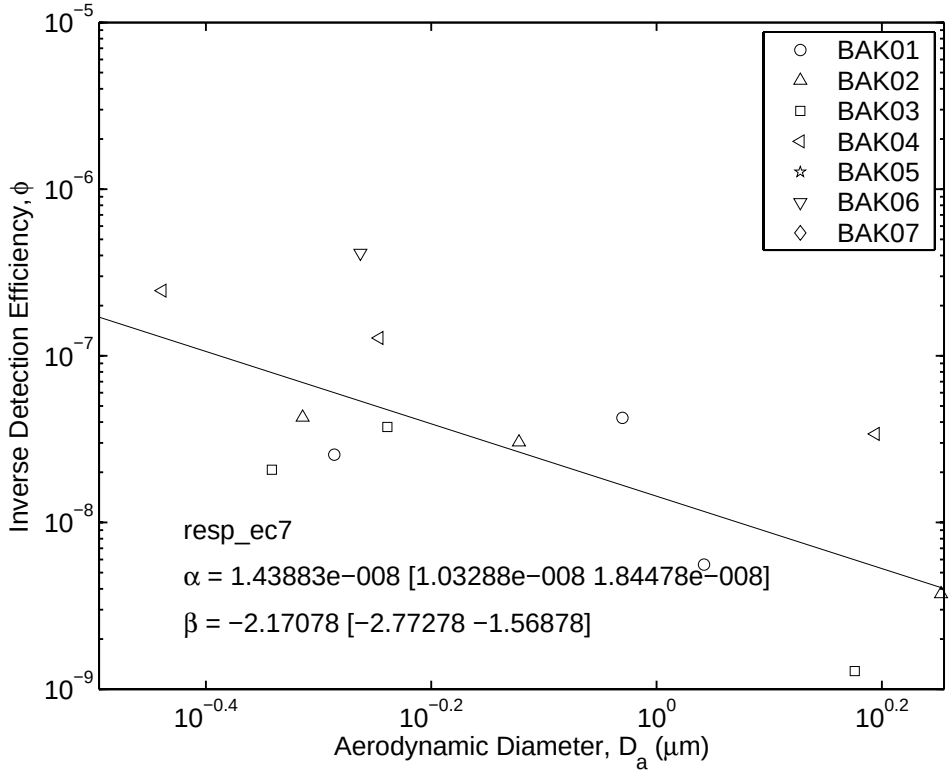

Figure 3.3: Inverse ATOFMS response efficiency, ϕ, versus aerodynamic diameter, D_a, for aerosol elemental carbon using response function EC7. Aerodynamic diameter is plotted at the average D_a weighted by the single particle response, R_{ik}. The line shows the best power law fit of the ATOFMS to impactor data. Text at lower left is single particle response function and fitted parameters; 95% confidence intervals are in brackets.

of single particle response functions that relate ATOFMS measurements with aerosol composition. For comparisons of particle mass, the mass of a spherical particle with uniform density yields good comparisons with impactor data. More difficult are response functions for aerosol components that are themselves operationally defined; such components are OC and EC.

In this work we tested response functions for OC based on classifications of particles detected by ATOFMS in studies of urban aerosol composition [Pastor et al., 2003]. The selected OC response function uses mass spectral peaks at $m/z = 27$ characteristic of $C_2H_3^+$ and excludes some mass spectra which resemble dust particles. Using this response function, the ATOFMS OC data compared well with the impactor data. We consider the comparison good since the scatter of the ATOFMS response for OC (see Figure 3.2) is similar to that for mass (see Figure 3.1).

In this work we also tested response functions for EC based on classifications of urban particles [Pastor et al., 2003]. The recommended EC response functions used the

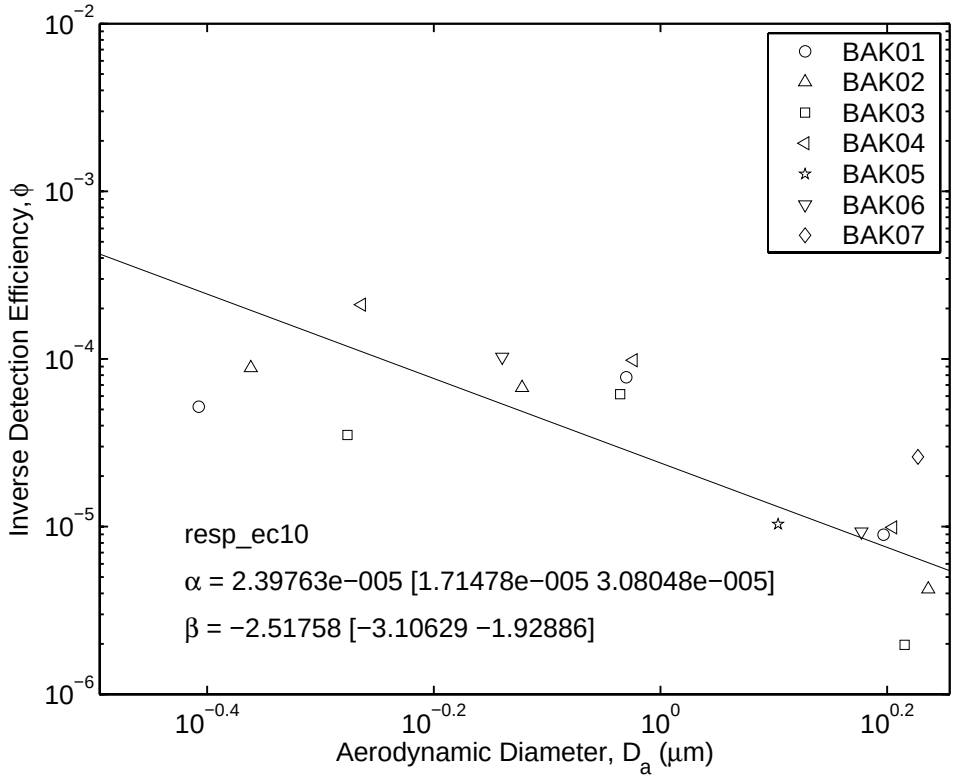

Figure 3.4: Inverse ATOFMS response efficiency, ϕ, versus aerodynamic diameter, D_a, for aerosol elemental carbon using response function EC10. Aerodynamic diameter is plotted at the average D_a weighted by the single particle response, R_{ik}. The line shows the best power law fit of the ATOFMS to impactor data. Text at lower left is single particle response function and fitted parameters; 95% confidence intervals are in brackets.

ratio of mass spectral response characteristic of EC (m/z = 36 and 60) to that for total carbon (m/z = 27, 36, 43, and 60). The recommended response function includes only those particles with significant signal at peaks characteristic of EC and excludes sea salt particles which have interfering mass spectral peaks. Using this response function, the ATOFMS EC data compared well with the impactor data. We consider the comparison good since the scatter of the ATOFMS response for EC (see Figure 3.4) is similar to that for mass (see Figure 3.1).

We have demonstrated a technique to develop response functions for the complex aerosol components OC and EC. This approach builds on the work of Bhave et al. [2002] in which response functions for inorganic ions were developed. The response functions are a compound signal from selected ions in mass spectra characteristic of the target analyte. The response functions also incorporate rules to exclude confounding particles which are of a type not likely to contain the analyte but whose mass spectra contain some peaks which overlap with those characteristic of the analyte. These rules are developed

by examination of a sample of single particle mass spectra. For the BIIS experiment, the most important confounding particle types were dust particles for OC and sea salt particles for EC. Other confounding particle types may be important in other studies.

A number of response functions for each analyte were developed and tested by comparison of scatter with respect to the reference sampler measurements. The goodness of fit for the response functions was evaluated qualitatively; recommended response functions had scatter approximately equal to that for the comparison of ATOFMS data with aerosol mass concentration. The mass response function is based only on particle size, not mass spectral data, and so reflects uncertainty only in the transmission and detection of particles in the ATOFMS instruments. More quantitative measures of the goodness-of-fit for aerosol composition response functions are possible, but unjustified because uncertainties in transmission and detection will affect all response functions and response function performance with better precision than that for aerosol mass is likely coincidental.

Since uncertainty regarding particle transmission and detection limits the precision of all quantitative comparisons of ATOFMS and reference sampler data, additional research in this area may improve quantitative analysis of ATOFMS data. Possible research projects in this area include laboratory studies of the transmission and detection of particles with known size and composition. Possible atmospheric sampling work includes collection and analysis of collocated ATOFMS, scanning mobility particle sizer (SMPS), and aerodynamic particle sizer (APS) data. The Prather group has performed a number of such laboratory and field experiments.

Analyte	α_i	β_i
T96, Transportable ATOFMS, Allen et al. [2000a]		
Mass	2.133×10^3 [1.632–2.634 $\times 10^3$]	-5.527 [-6.388 – -4.666]
Mass	2.896×10^3 [4.143–1.649 $\times 10^3$]	-5.500 [-6.657 – -4.343]
T96, Laboratory ATOFMS, Allen et al. [2000a]		
Mass	4.999×10^3 [4.001–5.997 $\times 10^3$]	-3.236 [-3.756 – -2.716]
T96, Laboratory ATOFMS, Bhave et al. [2002]		
Mass	5.040×10^3 [3.850–6.320 $\times 10^3$]	-3.13 [-3.77 – -2.49]
Ammonium	1.260×10^{-6} [1.058–1.462 $\times 10^{-6}$]	-0.730 [-1.13 – -0.33]
Nitrate	2.369×10^{-6} [2.016–2.722 $\times 10^{-6}$]	-0.730 [-1.13 – -0.33]
SCOS97-V1, Laboratory ATOFMS, Bhave et al. [2002]		
Mass	1.450×10^3 [1.016–1.884 $\times 10^3$]	-3.90 [-4.42 – -3.38]
Ammonium	0.363×10^{-6} [0.305–0.421 $\times 10^{-6}$]	-1.50 [-1.90 – -1.10]
Nitrate	0.682×10^{-6} [0.580–0.783 $\times 10^{-6}$]	-1.50 [-1.90 – -1.10]
SCOS97-V2, Laboratory ATOFMS, Bhave et al. [2002]		
Mass	2.050×10^3 [1.426–2.674 $\times 10^3$]	-4.46 [-4.92 – -4.00]
Ammonium	0.513×10^{-6} [0.431–0.595 $\times 10^{-6}$]	-2.06 [-2.46 – -1.66]
Nitrate	0.964×10^{-6} [0.820–1.107 $\times 10^{-6}$]	-2.06 [-2.46 – -1.66]
SCOS97-N3, Laboratory ATOFMS, Bhave et al. [2002]		
Mass	5.130×10^3 [2.990–7.270 $\times 10^3$]	-4.68 [-5.72 – -3.64]
Ammonium	1.283×10^{-6} [1.077–1.488 $\times 10^{-6}$]	-2.28 [-2.68 – -1.88]
Nitrate	2.411×10^{-6} [2.052–2.770 $\times 10^{-6}$]	-2.28 [-2.68 – -1.88]
BIIS, Transportable ATOFMS, Present Study		
Mass	1.900×10^3 [1.620–2.179 $\times 10^3$]	-5.702 [-5.998 – -5.407]
Organic Carbon	1.743×10^{-7} [1.405–2.081 $\times 10^{-7}$]	-3.042 [-3.393 – -2.691]
Elemental Carbon	2.398×10^{-5} [1.715–3.080 $\times 10^{-5}$]	-2.518 [-3.106 – -1.929]

Table 3.1: Best Fit Parameters for Quantitative Comparison of ATOFMS and Impactor Data.

Chapter 4

Scaled ATOFMS Data

4.1 Background

The single particle response functions developed here using data from the intensive sampling periods can also be used to recreate time series of aerosol concentrations over the entire BIIS experiment from the ATOFMS data. The scaled ATOFMS data can then be compared with the impactor data used to develop the scaling functions, as well as independent aerosol measurements. Comparison of scaled ATOFMS data with independent aerosol measurements can be used to assess the accuracy and reliability of our approach to scale ATOFMS data. Directly comparable and independent aerosol data were not available for our earlier research to quantitatively analyze ATOFMS data; the first comparison of this type is presented below.

4.2 Method

Twenty-three aerosol samplers were deployed as part of the BIIS experiment [Dutcher et al., 1999]. Two of these instruments, the ATOFMS and UC Davis MOIs, have been discussed extensively above. Many of the other aerosol samplers were filter and denuder samplers which were usually operated on a 24-h sampling schedule. These 24-h aerosol concentration data provide poor temporal resolution in comparison with the scaled ATOFMS, and so few data points for comparison. More useful for comparison with scaled ATOFMS data are the continuous fine aerosol mass instruments, including the Continuous Aerosol Mass Monitor (CAMM), and two Beta Attenuation Monitors (BAMs).

The continuous fine aerosol mass data from the CAMM and BAM instruments were evaluated by the BIIS project team [Dutcher et al., 1999]. They found that both BAM instruments averaged over 24 h had good correlation ($R^2 \geq 0.99$) with $PM_{2.5}$ concentrations determined using a Federal Reference Method (FRM) sampler. Comparison of

averaged CAMM and FRM data also showed good agreement ($R^2 \geq 0.97$). Because CAMM data are unavailable for 19–21 Jan 1999, we choose to compare scaled ATOFMS data with hourly $PM_{2.5}$ mass as determined by the average of the two BAM instruments.

Aerosol carbon measurements were also made as part of the BIIS experiment. These included two filter-based methods, the Spiral Aerosol Speciation Sampler (SASS) and Sequential Filter Sampler (SFS) [Dutcher et al., 1999]. A comparison of results from these instruments showed good agreement for total carbon (TC) with $R^2 = 0.94$ and agreement within $\approx 10\%$. Comparison of these OC data for these instruments showed a systematic difference between the two measurements of $\approx 20\%$ with $R^2 = 0.91$. For the EC data, the systematic difference was $\approx 30\%$ with $R^2 = 0.80$. The authors attribute the poor agreement on OC and EC concentrations between the SASS and SFS instruments to different operational definitions of OC and EC.

An Aerosol Dynamics, Inc., (ADI) flash vaporization carbon analyzer [Lim et al., 2003] was also deployed at the BIIS sampling site. This instrument is capable of 1-h measurements of carbonaceous aerosols; however, at the time of the BIIS experiment, this instrument was still under development. The resulting carbonaceous aerosol data did not pass ADI's quality control checks and so are not considered reliable. We therefore use the 24-h SASS aerosol carbon results for comparison with the scaled ATOFMS data.

The single particle response functions can be used to estimate the continuous aerosol concentrations from the ATOFMS data as a function of particle size as

$$\hat{m}_{ij} = \frac{\text{BusyScale}_j}{V_j} \sum_{k \subset j} \phi_{ik}(D_{a,k})\, R_{ik} \tag{4.1}$$

where $\hat{m}_{ij}$ is the estimate of the aerosol concentration for species i and time period j. This equation is analogous to Equation 3.4.

4.3 Results and Discussion

ATOFMS data were scaled up to aerosol mass concentrations using the recommended response function (Equation 3.3) and fitted parameters, α_{mass} and β_{mass} (see Table 3.1). The scaled ATOFMS data are hourly aerosol mass concentrations based on all the particles in the size range $D_a = 0.1$–2.5 μm detected during the study (09–28 Jan 1999) and (see Figure 4.1). Note that the response function parameters were calculated from analysis of particles over the range $D_a = 0.32$–1.8 μm; we extend the size range of particles considered to include all the $PM_{2.5}$ particles detected by the ATOFMS. Plotted with the scaled ATOFMS data are fine aerosol mass concentrations as measured by collocated BAMs and impactors. The BAMs data are the 1-h averaged measurements from the two BAMs instruments. The impactor mass concentration data are the sum of MOI impactor stages 5 through 7 which collect particles in the size range $D_a = 0.32$–1.8 μm. Impactor samples were collected for between 1000 and 1800 (1630 on 23 Jan 1999).

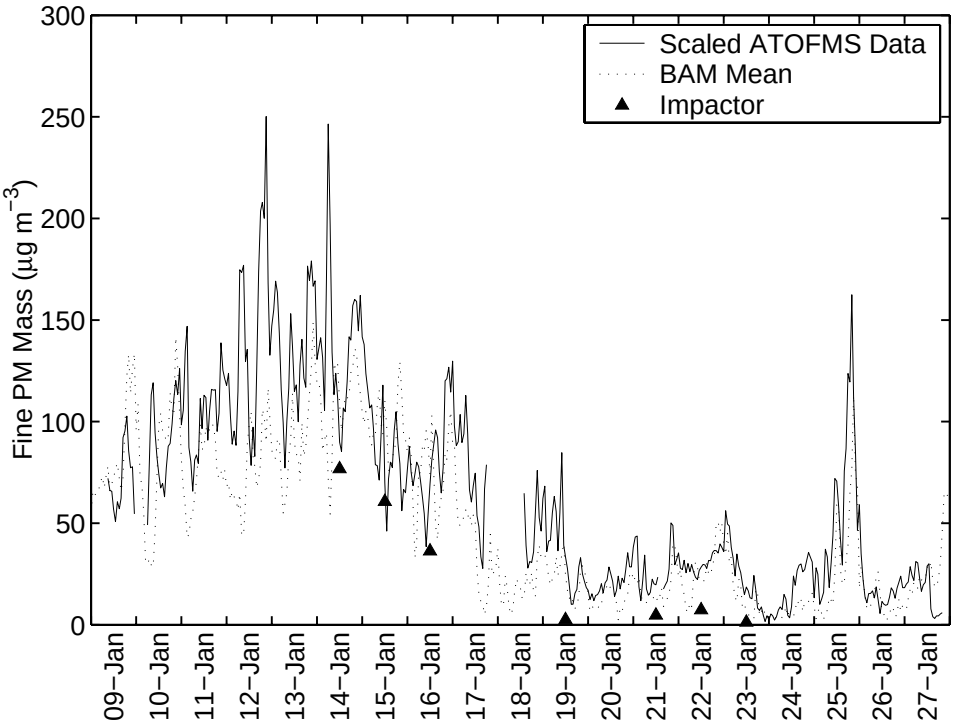

Figure 4.1: Fine aerosol mass concentrations from scaled ATOFMS data, beta attenuation monitors (BAMs) and a microorifice impactor (MOI). ATOFMS data are scaled 1-h collections of particles in the size range D_a = 0.1–2.5 μm. BAMs data are the 1-h averaged $PM_{2.5}$ measurements from two BAMs instruments [Dutcher et al., 1999]. Impactor mass concentration are particles in the range D_a = 0.32–1.8 μm collected for 8 h [Chung et al., 2001].

Agreement between the scaled ATOFMS data and the BAMs and MOI data are generally very good. The scaled ATOFMS mass concentration is greater than that measured using the impactors since the ATOFMS data includes particles in the size range D_a = 1.8–2.5 μm, which are not included in the MOI samples. Also note that, in the second half of the experiment when ambient aerosol concentrations were moderate, many of the gravimetric aerosol mass measurements were less than the uncertainty in the measurement, resulting in aerosol mass measurements less than the limit of detection for at least some stages of the impactor. In comparison with the BAMs data, the scaled ATOFMS data match very well in the second half of the study when $PM_{2.5}$ concentrations were generally less than 100 μg m^{-3}. In the first half of the study, scaled ATOFMS data follow the same temporal trends as the BAMs data but show differences of as much as a factor of three from the BAMs measurements. The noise in the scaled ATOFMS data may be due to noise in ATOFMS busy time estimates; as discussed in Chapter 2, a small uncertainty in busy time can have a large effect on BusyScale during times of high aerosol concentration. Over the entire study, the scaled ATOFMS data were generally

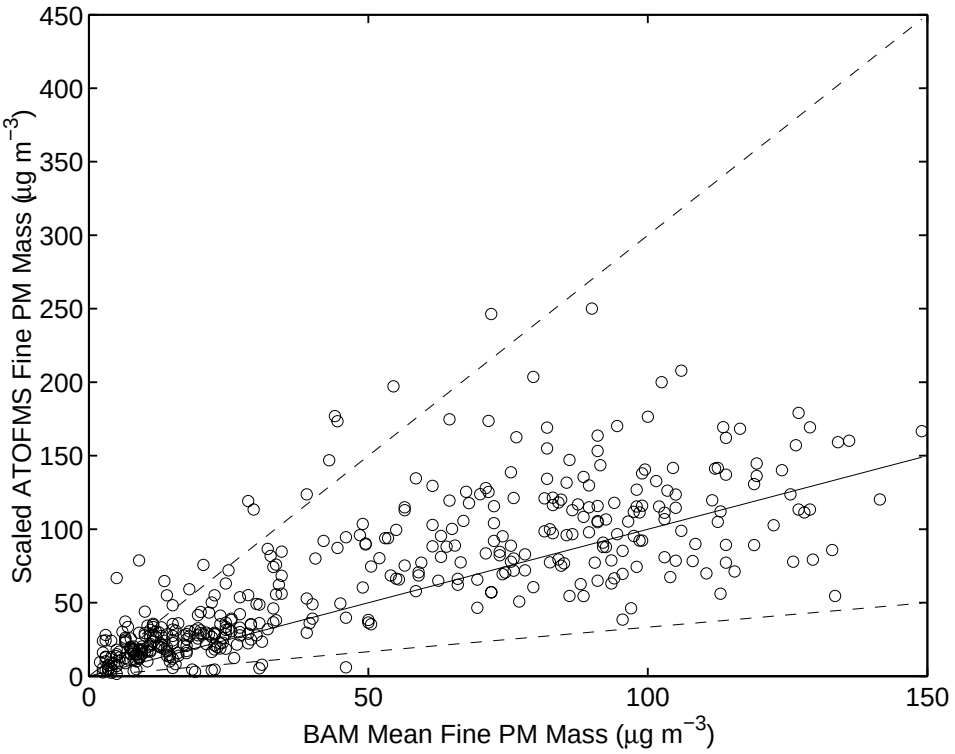

Figure 4.2: Comparison of fine aerosol mass concentrations from scaled ATOFMS data and beta attenuation monitors (BAMs). The solid line indicates the 1:1 match between scaled ATOFMS and BAMs data; the dashed lines indicate 3:1 and 1:3 matches between the data.

within a factor of three of the BAMs data (see Figure 4.2).

ATOFMS data were similarly scaled up to estimate aerosol OC and EC concentrations using the recommended response functions, OC7 and EC10, and fitted parameters, α_i and β_i (see Table 3.1). The scaled ATOFMS OC and EC data are hourly aerosol concentrations based on all the particles in the size range D_a = 0.1–2.5 μm detected during the study (09–28 Jan 1999) (see Figures 4.3 and 4.4). Note that the response function parameters were calculated from analysis of particles over the range D_a = 0.32–1.8 μm; we extend the size range of particles considered to include all the $PM_{2.5}$ particles detected by the ATOFMS. Plotted with the scaled ATOFMS data are fine aerosol OC and EC concentrations determined from impactor samples as well as independent measurements.

The scaled ATOFMS OC data track the impactor data for the seven days of impactor sampling. Note that the impactor data in Figures 4.3 and 4.4 are the sum of MOI impactor stages 5 through 7 which collect particles in the size range D_a = 0.32–1.8 μm between 1000 and 1800 (1630 on 23 Jan 1999). The amounts of OC detected on many of the impactor samples collected on 19, 21, 22, and 23 Jan 1999 were not greater than

the analytical uncertainty of the measurement. The imprecision of the impactor OC measurements in the later samples may have affected the ATOFMS OC data fitting so that the scaled ATOFMS OC data tend to be lower than the impactor data for the first three impactor samples.

Both the scaled ATOFMS data and impactor data are systematically lower than the SASS OC data. The summed impactor data are ≈ 1.5 times lower than the SASS OC data. In comparison with the impactor data, the SASS samples collected all particles smaller than 2.5 μm and were operated for 24-h, including the morning rush period, so that the impactor measurements are expected to be lower than the SASS measurements. Other explanations for the differences observed between the SASS and impactor OC results include sampling artifacts and differences in analytical procedures. Possible sampling artifacts include adsorption of gas-phase OC to the filter, and particle bounce and blow-off of collected OC from the aluminum impactor substrate. Since the impactor OC data are less than the SASS OC data, it is not surprising that the scaled ATOFMS OC data are also lower than the SASS OC data. The dotted line on Figure 4.3 shows the scaled ATOFMS OC data multiplied by 3; this additional scaling factor was arbitrarily selected. OC concentrations represented by this line generally follow the trend in daily SASS OC, including the period of high OC during 9–17 Jan 1999 and lower OC during 18–27 Jan 1999. The scaled ATOFMS OC data show the expected diel variations, with OC relatively higher during the morning and afternoon rush hours, and sometimes during the evening stagnation period. Note that the SASS data are the result of 24-h samples and are plotted at noon, when OC concentrations and scaled ATOFMS OC data are generally low.

The scaled ATOFMS EC data also track the impactor data for the seven days of impactor sampling. As with OC, the amounts of EC detected on many of the impactor samples collected on 19, 21, 22, and 23 Jan 1999 were not greater than the analytical uncertainty of the measurement. The imprecision of the impactor EC measurements in the later samples may have affected the ATOFMS EC data fitting so that the scaled ATOFMS EC data tend to be lower than the impactor data for the first three impactor samples.

Both the scaled ATOFMS data and impactor data are systematically lower than the SASS EC and aethelometer BC data. The summed impactor data are ≈ 15 times lower than the SASS EC data. This may be due to differences in the sizes and times of aerosol collection as well as sampling artifacts and differences in analytical procedures. Note that the impactor measurement shown in Figure 4.4 includes only particles in the size range D_a = 0.32–1.8 μm, and so omits samples which include most of the directly-emitted soot particles from diesel engines which have $D_a \approx 100$ nm. Since the impactor EC data are less than the SASS EC and aethelometer BC data, it is not surprising that the scaled ATOFMS EC data are also lower than both of the independent EC data sets. The dotted line on Figure 4.4 shows the scaled ATOFMS EC data multiplied by 30; this additional scaling factor was arbitrarily selected. EC concentrations represented by this line generally follow the trend in daily SASS EC, including the period of high EC during 9–

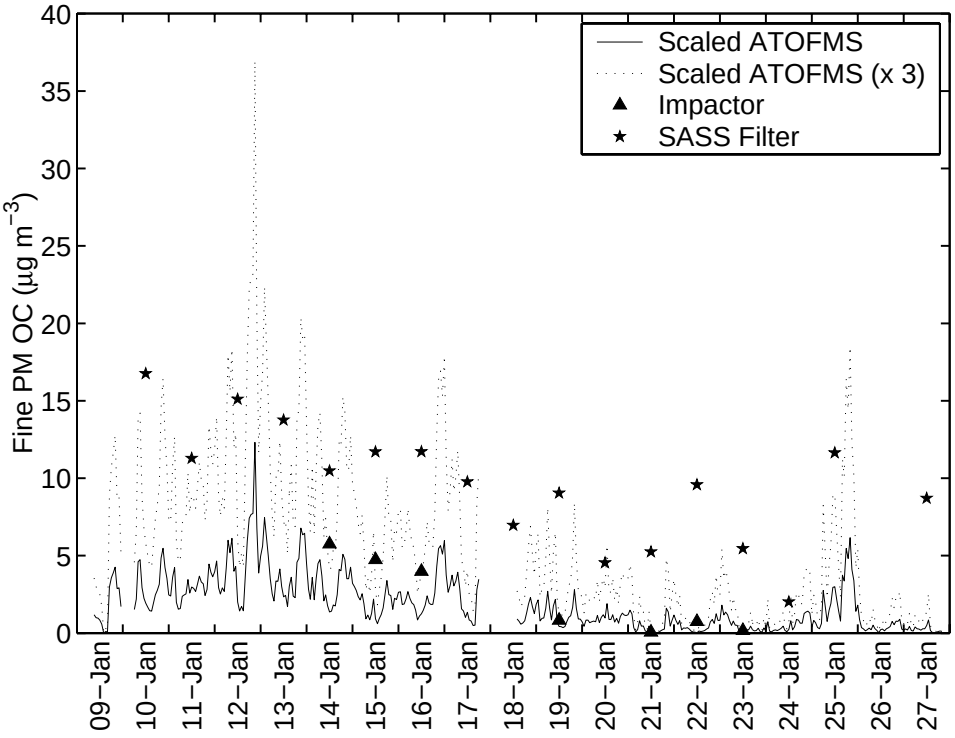

Figure 4.3: Fine aerosol OC concentrations from scaled ATOFMS data, a microorifice impactor (MOI), and SASS filter sampler. ATOFMS data are scaled 1-h collections of particles in the size range D_a = 0.1–2.5 μm. Impactor mass concentration are particles in the size range D_a = 0.32–1.8 μm collected for 8 h [Chung et al., 2001]. SASS filter data are from $PM_{2.5}$ samples collected midnight—midnight [Dutcher et al., 1999].

17 Jan 1999 and lower EC during 18–27 Jan 1999. The scaled ATOFMS EC data also show the expected diel variations with EC relatively higher during the morning and afternoon rush hours, and sometimes during the evening stagnation period. Note that the SASS data are the result of 24-h samples and are plotted at noon, when EC concentrations and scaled ATOFMS EC data are generally low.

4.4 Conclusions and Recommendations

Single particle response functions were used to recreate time series of aerosol concentrations over the entire BIIS experiment from the ATOFMS data. The scaled ATOFMS data were then compared with the reference sampler in order to assess the accuracy and reliability of our approach.

For $PM_{2.5}$ mass, the scaled ATOFMS data agreed well with both the impactor measurements and BAMs measurements. The scaled ATOFMS data agreed well with the

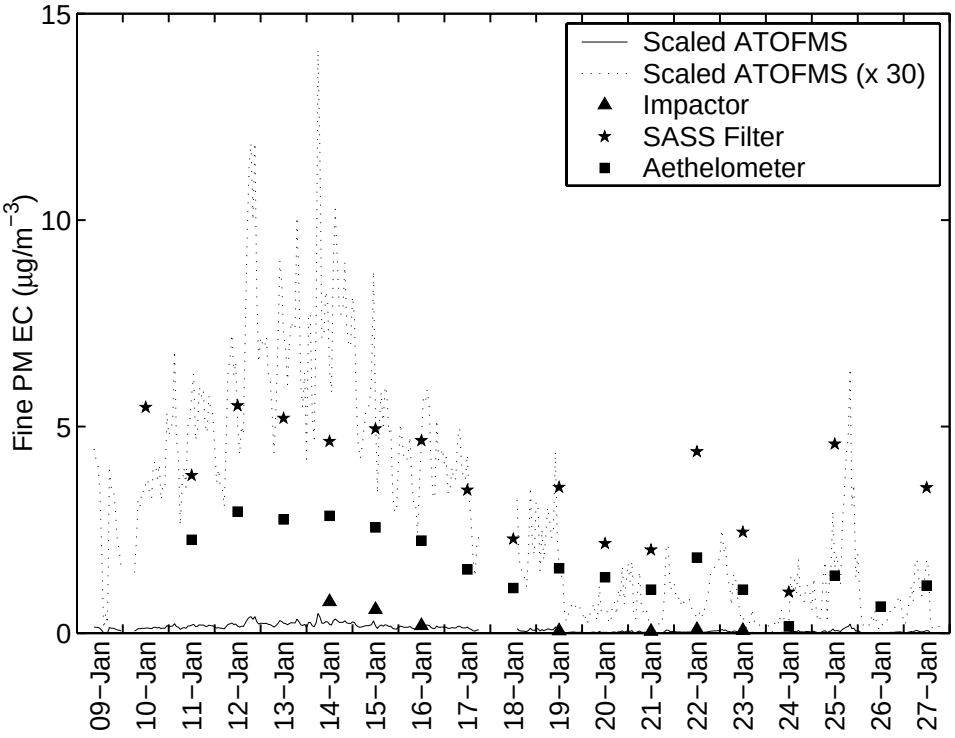

Figure 4.4: Fine aerosol EC concentrations from scaled ATOFMS data, a microorifice impactor (MOI), and SASS filter sampler. ATOFMS data are scaled 1-h collections of particles in the size range $D_a = 0.1$–2.5 μm. Impactor mass concentration are particles in the size range $D_a = 0.32$–1.8 μm collected for 8 h [Chung et al., 2001]. SASS filter data are from $PM_{2.5}$ samples collected midnight—midnight [Dutcher et al., 1999]. Aethelometer data are 24-h averaged black carbon measurements [Dutcher et al., 1999].

impactor measurements, except that scaled ATOFMS data were systematically higher than impactor data on low aerosol concentration days. This is likely due to large relative uncertainties in impactor mass measurements on these days since aerosol mass is measured gravimetrically as the difference in substrate weight before and after sampling. Impactor data below the method limit of detection were included here since low (uncertain) concentrations are also data that can be used to understand the ATOFMS operation.

The scaled ATOFMS data agreed well with independent 1-h $PM_{2.5}$ measurements using BAMs instruments. The scaled ATOFMS data followed the same diel trends that were observed in the BAMs measurements. Over the entire study, the scaled ATOFMS data generally agreed with the independent BAMs measurements within a factor of 3, so that scaled ATOFMS $PM_{2.5}$ data can be regarded as *semi-quantitative*.

For fine aerosol OC and EC, the scaled ATOFMS data agreed well with the impactor measurements. As with fine aerosol mass, low concentrations of fine aerosol OC and

EC were often below the limit of detection in the second half of the BIIS experiment. Impactor data below the method limit of detection were included here since low (uncertain) concentrations are also data that can be used to understand the ATOFMS operation.

The scaled ATOFMS data were systematically lower than independent filter-based measurements of fine aerosol OC and EC. It should be noted that systematic differences *between* collocated filter-based measurements were observed in this study and were attributed to differences in operational definitions of OC and EC. Further, the impactor reference sampler concentrations were systematically lower than filter-based OC and EC measurements by factors of approximately 1.5 and 15, respectively. It is therefore not surprising that the ATOFMS data scaled to match impactor data are also systematically lower than the independent filter-based measurements.

Differences between impactor and filter-based OC measurements may be due to differences in sampling time, operational definitions of OC, and sampling artifacts. In principle, ATOFMS data can be scaled to match the filter-based OC measurements. Multiplying the scaling factor from the comparison with impactor data by 3 gives a good match between the ATOFMS and filter-based OC measurements; a more precise scaling factor could be developed using a method similar to that used for the quantitative ATOFMS-impactor comparisons.

Differences between impactor and filter-based EC measurements are likely influenced by differences in sampling time, operational definitions of EC, and sampling artifacts; however the main difference results from exclusion of impactor stages which include most of the directly-emitted soot particles from diesel engines which have $D_a \approx 0.1$ μm. Impactor data for $D_a < 0.32$ μm were excluded because the ATOFMS used in the BIIS experiment detected few particles smaller than 0.32 μm. If the concentration of EC in particles in the size range $D_a = 0.32$–2.5 μm track the total fine aerosol EC concentration, then ATOFMS data can be scaled to fine aerosol EC.

The comparisons of scaled ATOFMS data with independent measurements of fine aerosol composition, especially those shown in Figures 4.3 and 4.4, provide the following lessons for future ATOFMS-reference sampler experiments, and for the development of ATOFMS:

- Samplers intended for use as reference samplers should have sampling protocols designed to detect aerosol analytes in quantities much greater than the limit of detection. For MOI samplers in conditions of moderate or low expected aerosol concentrations, sampling times should be extended to ensure collection of large aerosol samples. Alternatively, filter samplers which do not segregate samples by particle size, and so collect more material in each sample for the same flow rate, could be used as reference samplers; in this case concurrent particle size measurements are needed for quantitative comparison of ATOFMS data with both reference samplers.

- Continuous samplers, for example the Aerosol Dynamics, Inc., (ADI) flash vapor-

ization carbon analyzer [Lim et al., 2003] will be useful as reference samplers for quantitative comparison with ATOFMS data because 1-h measurements of aerosol composition provide a large number of data points for the comparisons. Data from the ADI carbon analyzer were not available from the BIIS experiment.

- Elemental carbon is mainly emitted as particles which have $D_a \approx 0.1$ μm. The ATOFMS instrument used in the BIIS experiment detected few particles smaller than D_a =0.32 μm, and so cannot detect much of the EC aerosol. Improvements to the ATOFMS inlet and particle detection technology are required to detect most EC particles. The good agreement of scaled ATOFMS data with impactor measurements in the size range D_a = 0.32–1.8 μm suggest that, once the ATOFMS instruments can detect particles smaller than D_a = 0.32 μm, the ATOFMS can determine semi-quantitatively fine aerosol EC concentrations.

Bibliography

Jonathan O. Allen, David P. Fergenson, Eric E. Gard, Lara S. Hughes, Bradley D. Morrical, Michael J. Kleeman, Deborah S. Gross, Markus E. Gälli, Kimberly A. Prather, and Glen R. Cass. Particle detection efficiencies of aerosol time of flight mass spectrometers under ambient sampling conditions. *Environ. Sci. Technol.*, 34:211–217, 2000a.

Jonathan O. Allen, Lara S. Hughes, Lynn G. Salmon, Paul R. Mayo, Robert J. Johnson, and Glen R. Cass. Characterization and evolution of primary and secondary aerosols during $PM_{2.5}$ and PM_{10} episodes in the South Coast Air Basin. Technical report, California Institute of Technology, 2000b. Coordinating Research Council Project A-22.

Prakash V. Bhave, Jonathan O. Allen, Bradley D. Morrical, David P. Fergenson, Glen R. Cass, and Kimberly A. Prather. A field-based approach for determining ATOFMS instrument sensitivities to ammonium and nitrate. *Environ. Sci. Technol.*, 36:4868–4879, 2002.

M. E. Birch and R. A. Cary. Elemental carbon-based method for monitoring occupational exposures to particulate diesel exhaust. *Aerosol Sci. Technol.*, 25:221–241, 1996.

A. Chung, J. D. Herner, and Michael J. Kleeman. Detection of alkaline ultrafine atmospheric particles at Bakersfield, California. *Environ. Sci. Technol.*, 35:2184–2190, 2001.

B. E. Dahneke and Y. S. Cheng. Properties of continuum source particle beams. I. Calculation methods and results. *J. Aerosol Sci.*, 10:257–274, 1979.

Morris H. DeGroot. *Probability and Statistics*. Addison-Wesley, Reading, MA, second edition, 1986.

Dabrina Dutcher, Albert Chung, Michael J. Kleeman, Alan E. Miller, Kevin D. Perry, Thomas A. Cahill, and Daniel P.Y. Chang. Instrument intercomparison study Bakersfield, CA 1998 - 1999. Technical report, University of California, Davis, 1999. Final Report on California Air Resources Board Contract Number 97-536.

David P. Fergenson. Personal communication. 1998. University of California, Riverside.

Eric E. Gard, Michael J. Kleeman, Deborah S. Gross, Lara S. Hughes, Jonathan O. Allen, Bradley D. Morrical, David P. Fergenson, Tas Dienes, Markus E. Gälli, Robert J. Johnson,

Glen R. Cass, and Kimberly A. Prather. Direct observation of heterogeneous chemistry in the atmosphere. *Science*, 279:1184–1187, 1998.

Eric E. Gard, Joseph E. Mayer, Bradley D. Morrical, Tas Dienes, David P. Fergenson, and Kimberly A. Prather. Real-time analysis of individual atmospheric aerosol-particles - design and performance of a portable ATOFMS. *Anal. Chem.*, 69:4083–4091, 1997.

Zhaozhu Ge, Anthony S. Wexler, and Murray V. Johnston. Laser desorption/ionizaton of single ultrafine multicomponent aerosols. *Environ. Sci. Technol.*, 32:3218–3223, 1998.

Deborah S. Gross, Markus E. Gälli, Philip J. Silva, and Kimberly A. Prather. Relative sensitivity factors for alkali metal and ammonium cations in single particle aerosol time-of-flight mass spectra. *Anal. Chem.*, 72:416–422, 2000.

Sergio A. Guazzotti, Jeffrey R. Whiteaker, David T. Suess, Keith R. Coffee, and Kimberly A. Prather. Real-time measurements of the chemical composition of size-resolved particles during a Santa Ana wind episode, California USA. *Atmos. Environ.*, 35:3229–3240, 2001.

Lara S. Hughes, Jonathan O. Allen, Prakash V. Bhave, Micheal J. Kleeman, Glen R. Cass, Don-Y. Liu, David P. Fergenson, Bradley D. Morrica, and Kimberly A. Prather. Evolution of atmospheric particles along trajectories crossing the Los Angeles basin. *Environ. Sci. Technol.*, 34:3058–3068, 2000.

Lara S. Hughes, Jonathan O. Allen, Michael J. Kleeman, Robert J. Johnson, Glen R. Cass, Deborah S. Gross, Eric E. Gard, Markus E. Gälli, Bradley D. Morrical, David P. Fergenson, Tas Dienes, Chrsitopher A. Noble, Don-Y. Liu, Philip J. Silva, and Kimberly A. Prather. The size and composition distribution of atmospheric particles in Southern California. *Environ. Sci. Technol.*, 33:3506–3515, 1999.

Lara S. Hughes, Jonathan O. Allen, Lynn G. Salmon, Paul R. Mayo, Robert J. Johnson, and Glen R. Cass. Evolution of nitrogen species air pollutants along trajectories crossing the Los Angeles area. *Environ. Sci. Technol.*, 36:3928–3935, 2002.

J. J. Huntzicker, R. L. Johnson, J. J. Shah, and R. A. Cary. . In G. T. Wolff and R. L. Klimisch, editors, *Particulate Carbon, Atmospheric Life Cycle*, pages 79–88. Plenum, New York, 1982.

Murray V. Johnston. Sampling and analysis of individual particles by aerosol mass spectrometry. *J. Mass Spectrom.*, 35:585–595, 2000.

David B. Kane and Murray V. Johnston. Size and composition biases on the detection of individual ultrafine particles by aerosol mass spectrometry. *Environ. Sci. Technol.*, 34:4887–4893, 2000.

H. J. Lim, B. J. Turpin, E. Edgerton, S. V. Hering, G. Allen, H. Maring, and P. Solomon. Semi-continuous aerosol carbon measurements: Comparison of Atlanta Supersite measurements. *J. Geophys. Res. - Atmospheres*, 108(D7):8419, 2003.

D. Y. Liu, D. Rutherford, M. Kinsey, and K. A. Prather. Real-time monitoring of pyrotechnically derived aerosol particles in the troposphere. *Anal. Chem.*, 69:1808–1814, 1997.

Don-Yuan Liu, Ryan J. Wenzel, and Kimberly A. Prather. Aerosol time-of-flight mass spectrometry during the Atlanta Supersite Experiment: 2. Measurements. *J. Geophys. Res.*, 108(D7):8426, 2003. DOI:10.1029/2001JD001562.

Bashir A. Mansoori, Murray V. Johnston, and Anthony S. Wexler. Quantitation of ionic species in single microdroplets by on-line laser desorption/ionization. *Anal. Chem.*, 66:3681, 1994.

Ann M. Middlebrook, Daniel M. Murphy, Shan-Hu Lee, David S. Thomson, Kimberly A. Prather, Ryan J. Wenzel, Don-Yuan Liu, Denis J. Phares, Kevin P. Rhoades, Anthony S. Wexler, Murray V. Johnston, Jos/'e L. Jimenez, John T. Jayne, Douglas R. Worsnop, Ivan Yourshaw, John H. Seinfeld, and Ricard C. Flagan. A comparison of particle mass spectrometers during the 1999 Atlanta Supersite Project. *J. Geophys. Res.*, 108(D7): 8424, 2003. DOI:10.1029/2001JD000660.

Kenneth R. Neubauer, Murray V. Johnston, and Anthony S. Wexler. On-line analysis of aqueous aerosols by laser desorption ionization. *Int. J. Mass Spectrom. Ion Processes*, 163:29–37, 1997.

Kenneth R. Neubauer, Murray V. Johnston, and Anthony S. Wexler. Humidity effects on the mass spectra of single aerosol particles. *Atmos. Environ.*, 32:2521–2529, 1998.

C. A. Noble and K. A. Prather. Real-time single-particle monitoring of a relative increase in marine aerosol concentration during winter rainstorms. *Geophys. Res. Letters*, 24: 2753–2756, 1997.

Christopher A. Noble and Kimberly A. Prather. Real-time measurement of correlated size and composition profiles of individual atmospheric aerosol particles. *Environ. Sci. Technol.*, 30(9):2667–2680, 1996.

Christopher A. Noble and Kimberly A. Prather. Real-time single particle mass spectrometry: A historical review of a quarter century of the chemical analysis of aerosols. *Mass Spectrometry Reviews*, 19:248–274, 2000.

Sylvia H. Pastor, Jonathan O. Allen, Lara S. Hughes, Prakash V. Bhave, Glen R. Cass, and Kimberly A. Prather. Ambient single particle analysis in Riverside, California, by aerosol time-of-flight mass spectrometry during SCOS97-NARSTO. *Atmos. Environ.*, 37:S239–S258, 2003.

William H. Press, Brian P. Flannery, Saul A. Teukolsky, and William T. Vetterling. *Numerical Recipes in C: The Art of Scientific Computing*. Cambridge University Press, second edition, 1992.

John H. Seinfeld and Spyros N. Pandis. *Atmospheric Chemistry and Physics: From Air Pollution to Global Change*. Wiley-Interscience, 1998.

Philip J. Silva and Kimberly A. Prather. Interpretation of mass spectra from organic compounds in aerosol time-of-flight mass spectrometry. *Anal. Chem.*, 72:3553–3562, 2000.

David S. Thomson, Ann M. Middlebrook, and Daniel M. Murphy. Thresholds for laser-induced ion formation from aerosols in a vacuum using ultraviolet and vacuum-ultraviolet laser wavelengths. *Aerosol Sci. Technol.*, 26:544–559, 1997.

Ryan J. Wenzel, Don-Yuan Liu, Eric S. Edgerton, and Kimberly A. Prather. Aerosol time-of-flight mass spectrometry during the Atlanta Supersite Experiment: 2. Scaling procedures. *J. Geophys. Res.*, 108(D7):8427, 2003. DOI:10.1029/2001JD001563.

Jeffrey R. Whiteaker and Kimberly A. Prather. Detection of pesticide residues on individual particles. *Anal. Chem.*, 75:49–56, 2003.

Jeffrey R. Whiteaker, David T. Suess, and Kimberly A. Prather. Effects of meteorological conditions on aerosol composition and mixing state in bakersfield, ca. *Environ. Sci. Technol.*, 36:2345–2353, 2002.

Appendix A

Copyrighted Materials Produced

One component of this project was the development of software code for analysis of ATOFMS data. This software development was part of a continuing effort begun in 1998 through which YAADA was developed. Copyrights to YAADA are held by the California Institute of Technology and Arizona Board of Regents; both institutions have permitted free public use of the software and underlying source code. Version 1.0 of YAADA was released to the public in December, 2000.

For the present project, new functions for the quantitative comparison of ATOFMS data with reference sampler data were added to YAADA. These will be included in the YAADA version 1.3 release. In addition, modification of existing functions in YAADA were needed for these analyses. These modifications were released as part of YAADA versions 1.1 (June 2002) and 1.2 (February 2003).

We will continue to provide the YAADA software including source code under a free license to the public. This arrangement will provide a resource to the atmospheric aerosol research community and is compatible with present contract between ASU and CARB.

Appendix B

Glossary

ATOFMS Aerosol Time-of-Flight Mass Spectrometry instrument designed by Prof. Kimberly Prather and her research group at University of California.

BIIS Bakersfield Instrument Intercomparison Study conducted at Bakersfield, CA, in January 1999.

$PM_{2.5}$ Particulate matter smaller than 2.5 μm.

PM_{10} Particulate matter smaller than 10 μm.

SCOS97 Southern California Ozone Study 1997.

YAADA Software toolkit to analyze single-particle mass spectral data. Acronym from "Yet Another ATOFMS Data Analyzer".

Appendix C

YAADA Updates

C.1 YAADA Version 1.1

YAADA version 1.1 was released on 30 June 2002. This update included functions to collect ATOFMS data binned by time and particle size into a table, PARTBIN, which is extensively used in the quantitative comparison calculations. This update also included new plots for data exploration and quality assurance. The complete release notes for this version follow.

1. Databases created under YAADA v0.93 and v1.0 will work under YAADA v1.10. The default structure for new databases created using v1.1 include new fields SpecGrav and Cluster in PART. The unused fields in SPEC (Noise, BaseLine, FitVoltage, FitZero) and PEAK (Width) have been removed. The updatedb function written by Prakash Bhave will update the database structure without redigesting the data.
2. Opendb switches between databases, a feature suggested by Prakash Bhave.
3. The aggregation operators now work only on spectra of one polarity. This change was suggested by Prakash Bhave and David Sodeman.
4. Run_query now accepts ids to limit searches.
5. PARTBIN is now a global table that is integrated with the rest of YAADA. Use get_pbidx to find indices in PARTBIN which correspond to Instrument-Time-Particle Size ranges. The collect_scos97 demonstrates how to create a PARTBIN table.
6. There are 3 new plot formats that are useful for data exploration and quality assurance. These are
   - plot_hit_miss is revised to use PARTBIN and runs much faster
   - plot_n_image plots number concentration as an image

- plot_busy_time plots on-line, off-line, and busy time

7. Msview and other programs generated an error when passed partid sets with only one particle. This is fixed in binary_search. Thanks to Keith Coffee for tracking down this bug.

8. Msview generated a warning message if you tried to display an empty set of partids. The new version does not show a warning message.

9. Prakash Bhave added a feature to @column/merge so columns of type CELL can now be merged.

10. There was a bug in the original combine function that caused errors when combining more than 3 sets of id objects. This is fixed.

C.2 YAADA Version 1.2

YAADA version 1.2 was released on 15 February 2003. This update included revisions to the PARTBIN table in which ATOFMS data binned by time and particle size are collected for analysis. This table is extensively used in the quantitative comparison calculations. This update also included an implementation of the ART-2a algorithm. We added this clustering algorithm so that particles could be classified as part of the quantitative comparisons. As part of this work, we found that this algorithm does not converge for reasonably sized data sets. As a result post processing of the ART-2a clusters is required for meaningful interpretation of the results. This postprocessing was deemed beyond the scope of the present research. The complete release notes for this version follow.

1. This version will work on databases generated using YAADA version 1.10. In order to use existing databases, install YAADA version 1.20, then run init to update study information. Do not clear the existing database.

2. The default file locations in init are now

c:/data/study/raw	Raw data in .inst, .pkl, .sem, and .sef files
c:/data/study/pk2	Data in .pk2 files
c:/data/study/ydb	YAADA database in .mat files

   The init function has also been revised to work better under unix.

3. This version includes a ratio search feature so that you can now do searches like

```
pid = run_query(''ratio(sum(area{23},area{39})) > 3'')
```

to find particles which have peaks at m/z = 23 that are more than 3 times the area of peaks at m/z = 39. The general syntax for the ratio operator is

```
ratio (AggOp1 (PeakColumn1 {mz1}), AggOp2 (PeakColumn2 {mz2}))
```

You can mix and match the AggOps (sum, min, max, mean, count, median) and the PeakColumns (Area, Height, Width, BlowScale) as needed. The ratio operator converts peak data into a single value for each particle. The value of the ratio for particles without data for the numerator *(AggOp1 (PeakColumn1 {mz1}))* is zero; for particles without data for the denominator *(AggOp2 (PeakColumn2 {mz2}))* is infinity. This yields intuitively reasonable results.

The ratio operator is more useful than relative searches which were implemented in YAADA v 0.93, but are not implemented in version 1.20. Relative searches had the syntax

```
sum(Area{23}) > sum(Area{39})
```

4. The interface for collect_partbin is changed so that the input InstCode, Start, Stop, DaMin, and DaMax must be vectors with one element for each Inst-Time-Size combination. A new function permute_partbin can be used to create these vectors by permuting all possible combinations of Inst-Time-Size. The script collect_scos97 shows how to use these functions for the SCOS97 dataset.

   Use collect_partbin when you need to create large groups of particles, e.g. particles grouped by impactor bins every hour. This function is optimized to create the groups efficiently and save them in a global table.

5. ART-2a clustering algorithm is included in this version of YAADA as cluster_art2a. This was based on David Fergenson's run_art2a function described in Fergenson et al., 1999. This function is called as

```
[PIDCell, PIDCount, OutWM] = cluster_art2a(InPID, Polarity, MaxMZ, ...
                                           Learning, Vigilance, ...
                                           StopCond, InWM, Verbose)
```

   The main changes from run_art2a are

   · Inner loop is rewritten so the program runs 3-4 times faster; it should also scale better for large partid sets.

- The resulting partids are output in a cell vector (PIDCell) that is sorted by the number of particles in the cluster. Otherwise, this is compatible with the output of run_art2a, so programs to analyze or display the clusters should still work.
- The number of particles in each cluster is output as PIDCount.
- The user can set the stop condition using StopCond. This can be based on the number of iterations (20 is the default maximum number of iterations). The new stop condition is NeuronChange which stops the run when the fraction of particles that change clusters between iterations is less than a set value (try 0.01). When looking for the NeuronChange stop condition, the function reports the fraction of particles that change each iteration.

6. This version runs under Matlab 6.5.
7. The get_column function returns values for duplicate IDs. In the earlier version, NaNs were returned for duplicate IDs.

C.3 YAADA Version 1.3

YAADA version 1.3 will be released after the final report for this project. This update will include the first public release of the quant package of functions used for the quantitative analyses discussed in this report. The quant package is coauthored by Jonathan O. Allen and Prakash V. Bhave. Dr. Bhave has already distributed two internal releases of this package to the coauthors and the Prather research group.

Appendix D

Attachment A - YAADA Manual version 1.2

Appendix E

Attachment B - Allen et al., 2000

Appendix F

Attachment C - Bhave et al., 2002